PHILOSOPHICAL TRANSACTIONS OF THE ROYAL SOCIETY A MATHEMATICAL, PHYSICAL & ENGINEERING SCIENCES

Asymptotic Calculation of Three-Dimensional Thin-Film Effects on Unsteady Hele-Shaw Fingering

S. Tanveer

Phil. Trans. R. Soc. Lond. A 1996 **354**, 1065-1097
doi: 10.1098/rsta.1996.0041

Asymptotic calculation of three-dimensional thin-film effects on unsteady Hele–Shaw fingering

By S. Tanveer

Mathematics Department, Ohio State University, Columbus, OH 43210, USA

Contents

An asymptotic calculation for the linear stability of a Hele–Shaw finger is presented in the limit $\epsilon \ll Ca \ll 1$ (ϵ being the gap to cell width ratio and Ca the capillary number) when three-dimensional thin-film effects are incorporated in the boundary conditions. Through formal asymptotic calculations, it is shown that as with the simpler idealized boundary conditions of McLean & Saffman (1981), there is only one branch of steady finger that is stable, while others are unstable. The spectrum of the linear stability operator is resolved through extraction of transcendentally small terms in ϵ.

Further, some aspects of the nonlinear initial value problem are investigated in the asymptotic limit $0 < \epsilon \ll 1$. When ϵ is set to zero in the equations, i.e. lateral curvature neglected, analytical evidence is presented to show that the initial value problem is ill-posed and is characterized by a finite time singularity on the finger boundary. Lateral curvature effects are expected to regularize the problem; nonetheless, calculations for special cases suggest that for $0 < \epsilon \ll 1$, extreme sensitivity of the dynamics occur due to the continual approach of complex singularities towards the physical domain, which is inherited from the $\epsilon = 0$ problem. These findings are consistent with highly unstable fingering observed experimentally for very small ϵ.

Phil. Trans. R. Soc. Lond. A (1996) **354**, 1065–1097
Printed in Great Britain

1. Introduction

The displacement of a more viscous fluid by a less viscous fluid in a Hele–Shaw cell has been the subject of intense interest in recent years due to mathematical analogies with dendritic crystal growth in the small Peclet number limit, deep cell shapes in directional solidification, electro-chemical deposition, etc. (see Pelce 1988; Kessler *et al.* 1988), though the original interest (Saffman & Taylor 1958) was sparked by analogies with displacement in a porous medium. While a controlled experiment in a Hele–Shaw cell is relatively easy to perform, this is not the case in some of the other mathematically related problems. In order to exploit the Hele–Shaw analogy to the fullest, especially for the time-dependent problem, it is important to have an adequate Hele–Shaw theory, where both qualititative and quantitative predictions can be checked against experiment.

The Hele–Shaw literature is extensive. Reviews by Saffman (1986), Bensimon *et al.* (1986) and Homsy (1986) summarize the state of affairs as of the mid-1980s. However, there has been considerable work since then, which has been reviewed from a number of different perspectives by Pelce (1988), Kessler *et al.* (1988), Howison (1992) and Tanveer (1991).

Almost all the the theory to date uses a relatively simple form of boundary condition, originally suggested by McLean & Saffman (1981) (henceforth referred to as the MS conditions), where the three-dimensional effects of a thin viscous film adjacent to the gap walls, as observed in the experiment, are ignored. While the theory developed with the MS boundary conditions still serves as a useful mathematical analogy to two-dimensional crystal growth and directional solidification, its relevance to Hele–Shaw experiments is not always clear. It is known that certain predicted theoretical features of the theory with MS boundary conditions are not in agreement with experiment (Tabeling *et al.* 1987).

For the steady finger, the boundary conditions were first discussed in a general way by Saffman (1982); later Park & Homsy (1985) developed effective two-dimensional boundary conditions that incorporate three-dimensional thin-film effects for small capillary number Ca, defined as $\mu U/T$, μ being the viscosity of the more viscous fluid (the viscosity of the less viscous being neglected), U is the steady finger velocity and T is the surface tension. Reinelt (1987*a*) extended the Park–Homsy calculations to arbitrary Ca by numerically determining some auxiliary functions that characterize the thin-film effects.

Using these Saffman–Park–Homsy–Reinelt (SPHR) conditions, Reinelt (1987*b*) calculated steady fingers that are in good agreement with experiment over a range in the ϵ–Ca parameter space. Schwartz & DeGregoria (1987) and Sarkar & Jasnow (1987) also used boundary conditions that incorporate three-dimensional effects in a partial manner to show agreement between their numerical calculations and experiments, though this agreement occurs over a narrower range in the parameter space than Reinelt's. Tanveer (1990) studied the asymptotic limit $\epsilon \ll 1$, $Ca \ll 1$ with $\epsilon^2 \ll Ca$. Numerically, this is a difficult limit to compute accurately since transcendentally small terms in ϵ have to be resolved. Various, though not exhaustive, relative orderings of ϵ and Ca were considered by Tanveer (1990). It was shown that only when $Ca \ll \mathcal{G}^{7/3} \ll 1$, the asymptotic scaling relation $\lambda = \frac{1}{2} + \text{const.}\, \mathcal{G}^{2/3}$ found for the MS boundary conditions (Combescot *et al.* 1986; Hong & Langer 1986; Shraiman 1986; Tanveer 1987*a*; Dorsey & Martin 1987; Combescot *et al.* 1987) holds, where λ is the

relative finger width and $\mathcal{G}$ is a reduced control parameter defined as

$$\mathcal{G} = \frac{\pi^2 \epsilon^2}{12\, Ca}. \tag{1.1}$$

However, this is outside the range of all experimental data to date. In the asymptotic limit $\epsilon \ll Ca \ll 1$, consistent with a few experimental data points, it was shown that a steady finger with $\lambda < \frac{1}{2}$ was possible, where

$$\frac{\lambda^2(1-\lambda)}{(1-2\lambda)} = k\frac{\epsilon}{Ca^{3/2}}. \tag{1.2}$$

For the first branch of solutions, the one with the smallest λ, $k = 2.832$†. The theoretical prediction of finger width using (1.2) appears to be in agreement with relevant experimental data; however, precise comparison has not been possible so far since Ca and ϵ are not sufficiently small in the existing experiments.

For the time-dependent problem, appropriate effective two-dimensional boundary conditions incorporating three-dimensional thin-film effects have also been developed by D. A. Reinelt, P. G. Saffman & S. Tanveer (unpublished work, 1993). Since the time scales associated with the narrow three-dimensional region are much smaller than a typical time scale of lateral interface motion, the pressure drop and viscous fluid leakage into the thin-film region remain functions of instantaneous curvature and normal speed in the lateral plane as for the steady state (Reinelt 1987*a*, *b*), at least to the leading order. In this paper, these boundary conditions are used to investigate the linear stability of the previously calculated steady states (Tanveer 1990), as well as to investigate the nonlinear initial value problem in the small ϵ limit.

The interest in the stability results in the small ϵ limit is more than theoretical. Based on the simplified MS boundary conditions, theoretical explanations of experimentally observed instability (Tabeling *et al.* 1987; Maxworthy 1987; Arneodo *et al.* 1989), for $\mathcal{G} \ll 1$ has been forwarded by Bensimon (1986) that rely on the observation that all but one branch of steady states is linearly unstable (Kessler & Levine 1986; Bensimon 1986; Tanveer 1987*b*), while in the limit $\mathcal{G} \to 0$ (or $\epsilon \to 0$), all branches of solution tend to the same Saffman–Taylor finger, whose width is one half that of the channel. As a result, the threshold for the onset of nonlinear stability must decrease with $\mathcal{G}$. However, when realistic three-dimensional thin film effects are included as discussed before, there is a regime in the parameter space where (1.2) holds and the λ on different branches (for which constant k is different) is significantly different when ϵ is the same order as $Ca^{3/2}$. Thus, the nonlinear instability mechanism proposed by Bensimon (1986) is absent in such cases when thin-film effects are included. Therefore, a proper explanation of the experimentally observed instability is desirable. In particular, there is no clear *a priori* reason to believe that when realistic three-dimensional thin-film effects are included, one branch of steady solutions remains stable for arbitrarily small $\mathcal{G}$. Based on a formal asymptotic calculation involving exponential asymptotics, we find in this paper that, as with the MS boundary conditions, one branch of steady solution is stable while others are unstable. Thus, we conclude that the instability mechanism is indeed nonlinear; this is consistent with our limited study of the initial value problem.

† In the earlier work (Tanveer 1990), a slightly inaccurate value of 2.776 was reported.

PHILOSOPHICAL TRANSACTIONS OF THE ROYAL SOCIETY A MATHEMATICAL, PHYSICAL & ENGINEERING SCIENCES

The interest in the initial value problem transcends questions on instability of a steadily translating finger mentioned in the last paragraph. It is clear from experiment (Tabeling *et al.* 1987; Maxworthy 1987; Arneodo *et al.* 1989) that for sufficiently small ϵ, highly ramified fractal-like structures can occur that hardly resemble a Saffman–Taylor finger. For the relatively simple MS boundary conditions, recent studies address the asymptotic limit $0 < \mathcal{G} \ll 1$ for special classes of analytic initial condition in a self-consistent manner (Tanveer 1993; Siegel *et al.* 1996). In the context of a time-dependent conformal map $z(\zeta, t)$ from a standard domain (interior of a unit circle or semicircle) to the physical flow domain, it was shown that for $\mathcal{G} = 0$, initial singularities, regardless of their nature, move towards $|\zeta| = 1$. Some types of these singularities impinge $|\zeta| = 1$ in finite time leading to interfacial cusps and corners, while others continually approach it exponentially in time. For $\mathcal{G}$ very small but nonzero, singularities are seen to be transformed; nonetheless, their leading-order motion in many cases is found to be the same as for a singularity of the $\mathcal{G} = 0$ problem until the singularity comes very close to the physical domain. As much as an initial interface is describable by the class of analytic initial conditions, it was pointed out that the motion of singularities towards $|\zeta| = 1$ is the fundamental reason for the chaotic dependence of the evolution on the initial interface shape. For instance, if we take two initial conditions $z^1(\zeta, 0)$ and $z^2(\zeta, 0)$ so that $z^1(\zeta, 0) - z^2(\zeta, 0) = \delta_1/(\zeta^2 + \delta_2^{-1})$; then by choosing δ_1 or δ_2 small enough, the initial interface shapes can be made experimentally indistinguishable since only the behaviour of the conformal map on $|\zeta| = 1$ is relevant to determining boundary shapes. Nonetheless, the initial singularity distribution in $|\zeta| > 1$ is different and, at later times when singularities approach $|\zeta| = 1$, the indentations on the interface will be quite different in the two cases. Realizing that a generic initial condition can have singularities at arbitrarily large distances from $|\zeta| = 1$, their continual approach towards $|\zeta| = 1$ helps explains the observed behaviour in numerical simulation for sufficiently small $\mathcal{G}$ (or small ϵ) (see, for example, DeGregoria & Schwartz 1986), where instead of a steady finger, a continual sequence of apparently random tip splitting events leaves behind a complicated pattern. The validity of this explanation for the actual experimental observations can be questioned since the MS boundary conditions are known to be unrealistic simplifications (Tabeling *et al.* 1987). That is addressed in the second part of the paper by considering the nonlinear initial value problem in the relevant asymptotic limit $\epsilon \ll 1$, where Ca need not be small. In particular, when we formally set $\epsilon = 0$ in our evolution equations, we find that the initial value problem is ill posed, in accordance with similar results for the MS boundary conditions (Howison 1986*a*, *b*). However, unlike the case with MS boundary conditions, not all singularities preserve their form in time. When $\epsilon \neq 0$, but is much less than unity, calculations for special form of singularities in $|\zeta| > 1$ show that transformed singularities also subsequently move towards $|\zeta| = 1$, similar to that for the MS boundary conditions. The results clearly show that even with realistic thin-film effects, the dynamics of complex singularities can explain the continuous time-evolving features of a finger in much the same way as for the MS boundary conditions (Tanveer 1993), though the quantitative details are different and generally far more complicated.

The paper is arranged as follows. Section 2 contains the mathematical formulation used in the linear stability analysis. Section 3 contains the details of the analytical linear stability calculations. Section 4 is a study of some analytical features of the initial value problem; the formulation used in that section is close to the earlier study

PHILOSOPHICAL TRANSACTIONS OF THE ROYAL SOCIETY A MATHEMATICAL, PHYSICAL & ENGINEERING SCIENCES

(Tanveer 1993) with the MS boundary conditions. Section 5 concludes the paper with a summary of the findings.

2. Mathamatical formulation

We consider a finger moving through a Hele–Shaw cell, as shown in figures 1 and 2, in the lateral and transverse planes, respectively. The cell has a gap width of b in the $\hat{z}$-direction, a cell width of $2a$ in the y-direction and is infinite in the x-direction. The aspect ratio $\epsilon = b/(2a)$ is assumed to be a small parameter. In the region away from the interface edge, the length scale for the lateral coordinates x and y is taken to be a. The velocities are scaled by U, the velocity of the steady finger and the pressure is scaled by $4\mu Ua/b^2$.

As the finger moves through the Hele–Shaw cell, a thin film is left behind next to the walls in region III occupied by the advancing finger. Its thickness is determined from the local solutions near the interface edge (in region II of figures 1 and 2). As discussed in Reinelt (1987*a*, *b*) within the context of a steady state, it is not necessary to solve a differential equation for the evolution of the laid-down thin film. The leveling of this film occurs over a very long scale and can be neglected. As shown by D. A. Reinelt, P. G. Saffman & S. Tanveer (unpublished work, 1993), since the time scale associated with the narrow gap direction is small compared to that of a typical disturbance in the lateral plane, it can be assumed that, to the leading order, the leakage of fluid into the thin-film region and the pressure drop across the relatively narrow region (region II) where three-dimensional effects are important is determined by the instantaneous normal velocity $U_{\rm n}$ of the interface (in the laboratory frame) and the curvature $\bar{C}$ in the lateral plane in the same way as for the steady state (Reinelt 1987*a*, *b*). In the asymptotic limit of $\epsilon \to 0$, the three-dimensional flow region (region II in the figures 1 and 2) shrinks in size relative to an interfacial length scale in the lateral plane. It is then possible to account for three-dimensional thin-film effects through effective boundary conditions on an idealized two-dimensional interface bounding a two-dimensional flow in region I. The pressure jump across region II (see figure 1) becomes a condition on the pressure in region I at the idealized two-dimensional interface in the lateral plane in the form

$$\bar{p} = \frac{\epsilon}{Ca}\kappa = \frac{\epsilon}{Ca}[\kappa^0(Ca\,U_{\rm n}) + \epsilon\bar{C}\kappa^1(Ca\,U_{\rm n})], \tag{2.1}$$

where κ^0 and κ^1, as functions of their argument, have been determined before (Reinelt 1987*a*, *b*) and $U_{\rm n}$ is the normal velocity of the interface in the laboratory frame of reference.

The movement of the more viscous fluid from region I to region III (see figures 1 and 2) is accounted for by the following kinematic condition at the two-dimensional idealized interface:

$$u_{\rm n} = U_{\rm n}[1 - m], \tag{2.2}$$

where $u_{\rm n}$ is the normal component of fluid velocity at the interface in the lab. frame, and

$$m = [m^0(Ca\,U_{\rm n}) + \epsilon\bar{C}m^1(Ca\,U_{\rm n})], \tag{2.3}$$

where the functions m^0 and m^1 have also been determined by Reinelt (1987*a*, *b*). Note that if the thin-film thickness m were zero, as assumed in the MS boundary condition, (2.2) is simply a statement that the normal velocity of a particle on the interface is the same as the normal fluid velocity.

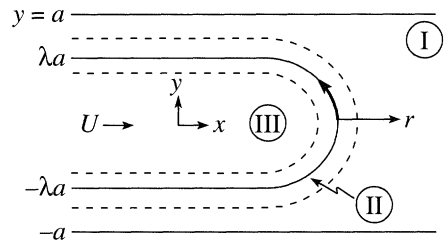

Figure 1. Hele–Shaw flow in the lateral $(x$–$y)$ plane. The dotted lines denote the boundary of region II, where three-dimensional effects are important. The curved solid line indicates the projection of the steady interface into the x–y plane.

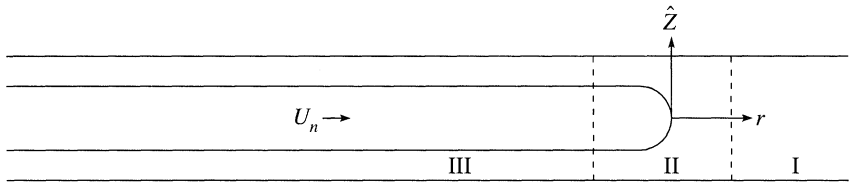

Figure 2. View from the transverse $(r$–$\hat{z})$ plane, where r is the normal distance from the curved solid line of figure 1.

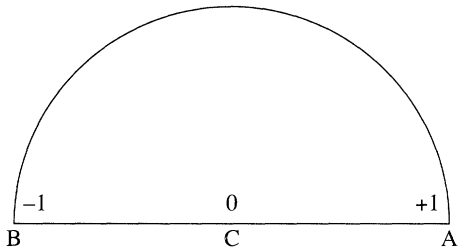

Figure 3. Unit semicircle in the ζ-plane.

Let us denote the argument of the functions κ^0, κ^1, m^0 and m^1 in (2.1) and (2.3) by $Ca_{\rm n}$. In the asymptotic limit of $Ca_{\rm n} \to 0$, following Bretherton's work (1961) in a mathematically similar problem of the motion of a bubble in a long narrow tube, Reinelt (1987a, b), following earlier work of Park & Homsy (1985), has determined

$$\kappa^0(Ca_{\rm n}) = \text{const.} - 3.878\, Ca_{\rm n}^{2/3} + O(Ca_{\rm n}), \tag{2.4}$$

$$\kappa^1(Ca_{\rm n}) = -\tfrac{1}{4}\pi + 4.153\, Ca_{\rm n}^{2/3} + O(Ca_{\rm n}), \tag{2.5}$$

$$m^0(Ca_{\rm n}) = 1.3375\, Ca_{\rm n}^{2/3} + O(Ca_{\rm n}), \tag{2.6}$$

$$m^1(Ca_{\rm n}) = -1.3375\tfrac{1}{4}\pi\, Ca_{\rm n}^{2/3} + O(Ca_{\rm n}). \tag{2.7}$$

The constant in (2.4) is dynamically unimportant and will be dropped since this is equivalent to absorbing an additive constant in the pressure $\bar{p}$ in (2.1), which does not effect the fluid or interface velocities.

For the linear stability analysis, it is convenient to move to the frame of the steady finger, which translates to the right with velocity U with respect to the laboratory frame. Consider the conformal map $z(\zeta, t)$ that maps the interior of the unit semicircle in the ζ plane, as shown in figure 3, to the physical flow domain in the $z = x + {\rm i}y$ plane shown in figure 4 such that $\zeta = 0$ corresponds to $z = +\infty$ and $\zeta = \pm 1$ corresponds to points $z = -\infty \pm {\rm i}$. We decompose the conformal mapping

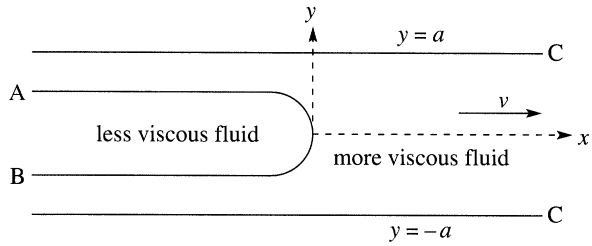

Figure 4. Rectilinear Hele–Shaw flow viewed in the lateral $z = x + \mathrm{i}y$ plane.

function into

$$z = -\frac{2}{\pi}\ln\zeta + \frac{2}{\pi}(1-\lambda)\ln(\zeta^2-1) - \mathrm{i}(1-2\lambda) + \frac{2}{\pi}f(\zeta,t). \tag{2.8}$$

It is well known that for the fluid motion in region I, the pressure field is approximately two dimensional and the narrow gap averaged velocity $(\bar{u},\bar{v}) = -\frac{1}{3}\nabla p$. From incompressibility of fluid flow, $\bar{p}$ must be harmonic. It follows that there exists a harmonic velocity potential $\phi(x,y) = -\frac{1}{3}\bar{p}$ such that the average velocity in the x–y plane is given by $(\bar{u},\bar{v}) = \nabla\phi$. Corresponding to this velocity potential, there exists a complex velocity potential W with $\phi = \mathrm{Re}\,W$. We consider W as an analytic function of ζ at each time and decompose it into

$$W = \frac{2}{\pi}(1-\lambda+\alpha)\ln\zeta - \frac{2}{\pi}(1-\lambda)\ln(\zeta^2-1) + \frac{2}{\pi}g(\zeta,t). \tag{2.9}$$

In order that the finger width does not vary with time, λ is independent of time. However, α in (2.9), which is proportional to the total fluid leakage into region III, is allowed to depend on time t. In terms of the conformal mapping function, it is easy to check that the normal component of the fluid velocity at the interface is given by

$$u_{\mathrm{n}} = n_x - \frac{1}{|z_\zeta|}\mathrm{Re}[\zeta W_\zeta], \tag{2.10}$$

where n_x is the x component of a unit normal at the interface and is determined from

$$n_x = -\frac{1}{|z_\zeta|}\mathrm{Re}[\zeta z_\zeta]. \tag{2.11}$$

Also, in the laboratory frame of reference, the normal velocity of a particle on the interface in the lateral plane (figure 4) is given by

$$U_{\mathrm{n}} = n_x - \frac{1}{|z_\zeta|}\mathrm{Re}[\zeta^* z_\zeta^* z_t]. \tag{2.12}$$

The kinematic boundary condition (2.2) can then be written as

$$\frac{2}{\pi}\mathrm{Re}[\zeta g_\zeta] = -m\,\mathrm{Re}[\zeta z_\zeta] - \frac{2\alpha}{\pi} + \mathrm{Re}[\zeta^* z_\zeta^* z_t](1-m) \tag{2.13}$$

on $|\zeta| = 1$, while the lateral plane curvature $\bar{C}$ is given by

$$\bar{C} = -\frac{1}{|z_\zeta|}\mathrm{Re}\left[1 + \frac{\zeta z_{\zeta\zeta}}{z_\zeta}\right]. \tag{2.14}$$

In (2.9), α is determined by

$$2\alpha = -\int_0^\pi \mathrm{d}\nu\, m y_\nu + \int_0^\pi (1-m)\,\mathrm{Re}[\zeta^* z_\zeta^* z_t]\,\mathrm{d}\nu. \tag{2.15}$$

From (2.15), it follows that if we require $\operatorname{Im} g \to 0$ as $\nu \to 0$ on the semicircular arc $\zeta = e^{i\nu}$, then $\operatorname{Im} g \to 0$ as $\nu \to \pi$. The dynamic pressure boundary condition (2.1) can be written as

$$\frac{2}{\pi} \operatorname{Re}[f + g] = -\frac{\epsilon}{3\, Ca} \kappa \tag{2.16}$$

on $|\zeta| = 1$. Since $\operatorname{Im} z = \pm 1$ on the walls which are also streamlines, it follows that on the real diameter of the unit ζ semicircle,

$$\operatorname{Im} f = 0, \tag{2.17}$$

$$\operatorname{Im} g = 0. \tag{2.18}$$

Equations (2.13) and (2.16)–(2.18) determine the evolution of f and g, once they are appropriately specified initially. It is to be noted that z, W and its derivatives that appear in these equations are determined from f and g through (2.8) and (2.9).

For a steady state, $z_t = 0$; consequently, the right-hand side of the kinematic equation (2.13) is simplified, as is the expression for U_{n} in (2.12). From this point onwards, the superscript 's' will correspond to a steady state. It is clear that the steady state function z^{s} and W^{s} satisfy the following conditions:

$$z^{\mathrm{s}}(\zeta) = -\frac{2}{\pi} \ln \zeta + \frac{2}{\pi}(1-\lambda) \ln(\zeta^2 - 1) - \mathrm{i}(1 - 2\lambda) + \frac{2}{\pi} f^{\mathrm{s}}(\zeta), \tag{2.19}$$

$$W^{\mathrm{s}}(\zeta) = \frac{2}{\pi}(1 - \lambda + \alpha^{\mathrm{s}}) \ln \zeta - \frac{2}{\pi}(1-\lambda) \ln(\zeta^2 - 1) + \frac{2}{\pi} g^{\mathrm{s}}(\zeta), \tag{2.20}$$

where on $|\zeta| = 1$,

$$\frac{2}{\pi} \operatorname{Re}[f^{\mathrm{s}} + g^{\mathrm{s}}] = -\frac{\epsilon}{3\, Ca} \kappa^{\mathrm{s}}, \tag{2.21}$$

$$\operatorname{Re}[\zeta g^{\mathrm{s}}_{\zeta}] = -\alpha^{\mathrm{s}} - \operatorname{Re}[\zeta(f^{\mathrm{s}}_{\zeta} + h)] m^{\mathrm{s}}. \tag{2.22}$$

The functions κ^{s} and m^{s} are given by

$$\kappa^{\mathrm{s}} = \kappa^0(Ca\, n^{\mathrm{s}}_x) + \epsilon \kappa^1(Ca\, n^{\mathrm{s}}_x) \bar{C}^{\mathrm{s}}, \tag{2.23}$$

$$m^{\mathrm{s}} = m^0(Ca\, n^{\mathrm{s}}_x) + \epsilon m^1(Ca\, n^{\mathrm{s}}_x) \bar{C}^{\mathrm{s}}, \tag{2.24}$$

where

$$n^{\mathrm{s}}_x = -\frac{\operatorname{Re}[\zeta(f^{\mathrm{s}}_{\zeta} + h)]}{|f^{\mathrm{s}}_{\zeta} + h)|}, \tag{2.25}$$

$$\bar{C}^{\mathrm{s}} = -\frac{\pi}{2|h + f^{\mathrm{s}}_{\zeta}|} \operatorname{Re}\left[1 + \zeta \frac{f^{\mathrm{s}}_{\zeta\zeta} + h_{\zeta}}{f^{\mathrm{s}}_{\zeta} + h}\right], \tag{2.26}$$

$$h(\zeta) = \frac{1 + q^2 \zeta^2}{\zeta(\zeta^2 - 1)}, \tag{2.27}$$

$$q^2 = 1 - 2\lambda. \tag{2.28}$$

In a standard manner, appropriate for the linear stability analysis, we decompose each of the functions $z(\zeta, t)$ and $W(\zeta, t)$ as follows:

$$z = z^{\mathrm{s}} + \frac{2}{\pi} f^{\mathrm{u}}, \tag{2.29}$$

$$W = W^{\mathrm{s}} + \frac{2}{\pi} g^{\mathrm{u}} + \frac{2\alpha^{\mathrm{u}}}{\pi} \ln \zeta. \tag{2.30}$$

In addition $\alpha = \alpha^{\mathrm{s}} + \alpha^{\mathrm{u}}$. The superscript 'u' denotes the unsteady components. The linearized equations for f^{u} and g^{u} are then given by

$$\frac{2}{\pi}\,\mathrm{Re}[f^{\mathrm{u}} + g^{\mathrm{u}}] = -\tfrac{1}{3}\epsilon\kappa'(Ca\,n_x^{\mathrm{s}})(\delta n_x) - \frac{\epsilon^2}{3\,Ca}\kappa^1(Ca\,n_x^{\mathrm{s}})(\delta\bar{C}), \tag{2.31}$$

$$\begin{aligned}\frac{2}{\pi}\,\mathrm{Re}[\zeta g_\zeta^{\mathrm{u}}] = &- Ca\,m'(Ca\,n_x^{\mathrm{s}})(\delta n_x)\,\mathrm{Re}[\zeta z_\zeta^{\mathrm{s}}] - \frac{2}{\pi}m(Ca\,n_x^{\mathrm{s}})\,\mathrm{Re}[\zeta f_\zeta^{\mathrm{u}}]\\ &-\epsilon m^1(Ca\,n_x^{\mathrm{s}})\,\mathrm{Re}[\zeta z_\zeta^{\mathrm{s}}](\delta\bar{C}) - \frac{2}{\pi}\alpha_1 + \frac{2}{\pi}\,\mathrm{Re}[\zeta^* z_\zeta^{s^*} f_t^{\mathrm{u}}][1 - m(Ca\,n_x^{\mathrm{s}})]\end{aligned} \tag{2.32}$$

on $\zeta = \mathrm{e}^{\mathrm{i}\nu}$, where

$$\kappa'(Ca\,n_x^{\mathrm{s}}) = \kappa^{0'}(Ca\,n_x^{\mathrm{s}}) + \epsilon\bar{C}^{\mathrm{s}}\kappa^{1'}(Ca\,n_x^{\mathrm{s}}), \tag{2.33}$$

$$m'(Ca\,n_x^{\mathrm{s}}) = m^{0'}(Ca\,n_x^{\mathrm{s}}) + \epsilon\bar{C}^{\mathrm{s}}m^{1'}(Ca\,n_x^{\mathrm{s}}), \tag{2.34}$$

where primes indicate derivatives with respect to the argument. Further, in (2.31) and (2.32),

$$\delta n_x = -\frac{2}{\pi}\frac{\mathrm{Re}[\zeta f_\zeta^{\mathrm{u}}]}{|z_\zeta^{\mathrm{s}}|} + \frac{2}{\pi|z_\zeta^{\mathrm{s}}|}\,\mathrm{Re}[\zeta z_\zeta^{\mathrm{s}}]\,\mathrm{Re}\left[\frac{f_\zeta^{\mathrm{u}}}{z_\zeta^{\mathrm{s}}}\right], \tag{2.35}$$

$$\delta\bar{C} = -\frac{2}{\pi|z_\zeta^{\mathrm{s}}|}\,\mathrm{Re}\left[\zeta\frac{\mathrm{d}}{\mathrm{d}\zeta}\left\{\frac{f_\zeta^{\mathrm{u}}}{z_\zeta^{\mathrm{s}}}\right\}\right] + \frac{2}{\pi|z_\zeta^{\mathrm{s}}|}\,\mathrm{Re}\left[1 + \zeta\frac{z_{\zeta\zeta}^{\mathrm{s}}}{z_\zeta^{\mathrm{s}}}\right]\mathrm{Re}\left[\frac{f_\zeta^{\mathrm{u}}}{z_\zeta^{\mathrm{s}}}\right]. \tag{2.36}$$

Equations (2.31) and (2.32), together with the condition $\mathrm{Im}\,f^{\mathrm{u}} = 0$ and $\mathrm{Im}\,g^{\mathrm{u}} = 0$ on the real diameter (i.e. ζ in $[-1, 1]$), constitute the linear stability equations for f^{u} and g^{u}. It may be noticed that no additional equation is necessary for α^{u} as it is determined by imposing the self-consistency requirement on (2.32) that

$$\int_0^\pi \mathrm{d}\nu\,\frac{\partial}{\partial\nu}\,\mathrm{Im}\,g^{\mathrm{u}}(\mathrm{e}^{\mathrm{i}\nu}) = 0.$$

A steady-state calculation to determine λ and the function f^{s} has been carried out before (Tanveer 1990) for $\epsilon \ll 1$ and $Ca \ll 1$ for various (though not exhaustive) relative orderings of the parameters ϵ and Ca. No constraint on λ arose from a regular perturbation expansion in powers of ϵ and Ca. Evidence was also presented (Tanveer 1990) to show that a perturbation expansion in powers of ϵ for $Ca = O(1)$ fails to select λ. Restrictions were found on λ by extracting exponentially small terms in ϵ and imposing on them appropriate conditions of symmetry. To determine the coefficients of exponentially small terms, following the earlier ideas of Pokrovskii & Khalatnikov (1961), Kruskal & Segur (1986) for ordinary differential equations and a similar procedure for the simpler MS boundary conditions (Combescot *et al.* 1986, 1987; Tanveer 1987), it is necessary to investigate the neighbourhood of points in $|\zeta| > 1$, where a regular perturbation expansion fails. The details of the inner equation analysis depends on the relative ordering of Ca and ϵ. Since our stability analysis is limited to $\epsilon \ll Ca \ll 1$ for which (1.2) holds, only the inner equation analysis presented in § 5 *c* of Tanveer (1990) is relevant here.

3. Linear stability problem

In the asymptotic limit $\epsilon \ll Ca \ll 1$, it is appropriate to consider a regular perturbation expansion for each eigenmode. It will be seen that even without any

constraints on the eigenvalues, such an expansion is valid everywhere on the finger boundary except near the tails $\zeta = \pm 1$, where a secondary inner expansion is necessary. We will then proceed to examine constraints on eigenvalues arising due to terms that are transcendentally small in $|\zeta| \leqslant 1$. This is effectively done by analytical continuation of the equations to the unphysical domain $|\zeta| > 1$. Our analysis so far is limited to eigenvalues σ for which $|\sigma| \ll \mathcal{G}^{-1/2}$. This assumption does not appear to be serious as far as our conclusion that one branch of solution is stable since numerical results (D. A. Reinelt, P. G. Saffman & S. Tanveer (unpublished work, 1993)) for non-zero $\mathcal{G}$ suggest that $\mathcal{G}^{1/2}\sigma$ tends to zero as $\mathcal{G}$ becomes smaller for any possibly unstable eigenvalue, at least up to the smallest $\mathcal{G}$ for which reliable computation was possible.

(*a*) *Regular perturbation expansion*

First, we consider the regular perturbation expansion for the linearized stability equations (2.31) and (2.32) for $\epsilon \ll 1$ and $Ca \ll 1$ in the form

$$f^{\mathrm{u}} = f_0^{\mathrm{u}} + f_1^{\mathrm{u}} + \cdots, \tag{3.1}$$

$$g^{\mathrm{u}} = g_0^{\mathrm{u}} + g_1^{\mathrm{u}} + \cdots. \tag{3.2}$$

Clearly, from (2.31) and (2.32), on $\zeta = \mathrm{e}^{\mathrm{i}\nu}$, we get

$$\mathrm{Re}[f_0^{\mathrm{u}} + g_0^{\mathrm{u}}] = 0, \tag{3.3}$$

$$\mathrm{Re}[\zeta g_{0_\zeta}^{\mathrm{u}}] = \mathrm{Re}\left[\zeta^* z_{0_\zeta}^{s^*} f_t^{\mathrm{u}}\right], \tag{3.4}$$

where the subscript zero on the steady stage function z^{s} corresponds to $\epsilon = 0$. In order to be consistent with (2.17) and (2.18), it is necessary for $\mathrm{Im}\, f_0^{\mathrm{u}} = 0$, $\mathrm{Im}\, g_0^{\mathrm{u}} = 0$ on the real diameter of the unit ζ semicircle.

The precise form of the next order correction f_1^{u} depends on more information on the relative ordering of ϵ and Ca than we are provided with. In order to cover all cases of this ordering, we found it best to impose the following boundary conditions on f_1^{u} and g_1^{u}:

$$\mathrm{Re}[f_1^{\mathrm{u}} + g_1^{\mathrm{u}}] = -\tfrac{1}{6}\epsilon\pi\kappa'(Ca\, n_x^0)(\delta n_{x^0}) - \frac{\pi\epsilon^2}{6\, Ca}\kappa^1(Ca\, n_x^0)(\delta\bar{C}_0) \tag{3.5}$$

$$\begin{aligned}\mathrm{Re}\left[\zeta g_{1_\zeta}^{\mathrm{u}} - \frac{2}{\pi}\left(\frac{\zeta^2+q^2)}{1-\zeta^2}\right) f_{1_t}^{\mathrm{u}}\right] \\ = -\, Ca\, \mathrm{Re}[\zeta h] m^{0'}(Ca\, n_x^0)(\delta n_{x^0}) - m^0(Ca\, n_x^0)\, \mathrm{Re}[\zeta f_{0_\zeta}^{\mathrm{u}}] \\ -\alpha_1^{\mathrm{u}} - \frac{2}{\pi}\,\mathrm{Re}\left\{\frac{\zeta^2+q^2}{1-\zeta^2} f_{0_t}^{\mathrm{u}}\right\} m^0(Ca\, n_x^0),\end{aligned} \tag{3.6}$$

where

$$\kappa'(Ca\, n_x^0) = \kappa^{0'}(Ca\, n_x^0) + \epsilon\kappa^{1'}(Ca\, n_x^0)\bar{C}^0, \tag{3.7}$$

$$n_x^0 = -\frac{1}{|h|}\,\mathrm{Re}[\zeta h], \tag{3.8}$$

$$\bar{C}^0 = -\frac{\pi}{2|h|}\,\mathrm{Re}\left[1 + \frac{\zeta h'}{h}\right], \tag{3.9}$$

$$\delta n_{x_0} = -\frac{1}{|h|}\,\mathrm{Re}[\zeta f^{\mathrm{u}}_{0_\zeta}] + \frac{\mathrm{Re}[\zeta h]}{|h|}\,\mathrm{Re}\left[\frac{f^{\mathrm{u}}_{0_\zeta}}{h}\right], \tag{3.10}$$

$$\delta C_0 = -\frac{\pi}{2|h|}\,\mathrm{Re}\left\{\zeta\frac{\mathrm{d}}{\mathrm{d}\zeta}\left[\frac{f^{\mathrm{u}}_{0_\zeta}}{h}\right]\right\} + \frac{\pi}{2|h|}\,\mathrm{Re}\left[1+\zeta\frac{h_\zeta}{h}\right]\mathrm{Re}\left[\frac{f^{\mathrm{u}}_{0_\zeta}}{h}\right]. \tag{3.11}$$

In order to be consistent with (2.17) and (2.18), it is necessary for $\mathrm{Im}\, f^{\mathrm{u}}_1 = 0$, $\mathrm{Im}\, g^{\mathrm{u}}_1 = 0$ on the real diameter.

Now, we determine f^{u}_0 and g^{u}_0. From (3.3) and (3.4),

$$\mathrm{Re}\left[\zeta f^{\mathrm{u}}_{0_\zeta} + \frac{2}{\pi}\left(\frac{\zeta^2+q^2}{1-\zeta^2}\right) f^{\mathrm{u}}_{0_t}\right] = 0. \tag{3.12}$$

As shown by Tanveer (1987*b*) (in the context of zero surface tension eigenmodes of the MS boundary conditions), for symmetric modes, (3.12) is equivalent to the differential equation

$$(\zeta^2-1)f^{\mathrm{u}}_{0_\zeta} - \frac{2}{\pi}\left(\frac{\zeta^2+q^2}{\zeta}\right) f^{\mathrm{u}}_{0_t} = -\frac{2}{\pi}q^2 f^{\mathrm{u}}_{0_t}(0,t)\left(\frac{1}{\zeta}+\zeta\right). \tag{3.13}$$

Note that the parameter $p^2 = -q^2$ was used in Tanveer (1987*b*). For the antisymmetric modes, it has been shown (Tanveer 1987*b*) that (3.12) is equivalent to the differential equation

$$(\zeta^2-1)f^{\mathrm{u}}_{0_\zeta} - \frac{2}{\pi}\left(\frac{\zeta^2+q^2}{\zeta}\right) f^{\mathrm{u}}_{0_t} = -\frac{2}{\pi}(1+q^2) f^{\mathrm{u}}_{0_t}(1,t). \tag{3.14}$$

With an assumed $\mathrm{e}^{\sigma t}$ time dependence, the symmetric eigenmodes for $\mathrm{Re}\,\sigma > 0$, $q^2 > 0$ are given by

$$f^{\mathrm{u}}_0 = -f^{\mathrm{u}}(0,t)\tilde{\sigma}q^2 H^{-1}(\zeta)\int_0^\zeta \mathrm{d}\zeta'\left(\frac{H(\zeta')(1+\zeta'^2)}{\zeta'(\zeta'^2-1)}\right), \tag{3.15}$$

while the antisymmetric eigenmodes for $\mathrm{Re}\,\sigma > 0$, $q^2 > 0$ are given by

$$f^{\mathrm{u}}_0 = -f^{\mathrm{u}}_0(1,t)\tilde{\sigma}(1+q^2)H^{-1}(\zeta)\int_0^\zeta \mathrm{d}\zeta'\left(\frac{H(\zeta')}{1-\zeta'^2}\right), \tag{3.16}$$

where

$$H(\zeta) = \zeta^{q^2\tilde{\sigma}}(1-\zeta^2)^{-\tilde{\sigma}(1+q^2)/2}, \tag{3.17}$$

with

$$\tilde{\sigma} = \frac{2}{\pi}\sigma. \tag{3.18}$$

The expressions (3.15) and (3.16) are also valid if $\mathrm{Re}\,\sigma = 0$, provided $\mathrm{Im}\,\sigma \neq 0$. When $\sigma = 0$, the corresponding eigenmode is a translation mode, with $f^{\mathrm{u}}_0 = \text{const.}$, $g^{\mathrm{u}}_0 = -f^{\mathrm{u}}_0$.

We notice that the eigenmodes (3.15) and (3.16) are well behaved at $\zeta = 0$, the apparent branch point singularity inside and outside the integrals cancel out. However, there are branch point singularities at $\zeta = \pm 1$ unless $\tilde{\sigma}\frac{1}{2}(1+q^2)$ is a positive integer. For $\mathrm{Re}\,\sigma < 0$, the branch points are unacceptable if we restrict ourselves to the class of disturbances that vanish at the finger tails. Thus, the spectrum is the entire right half-plane $\mathrm{Re}\,\sigma \geqslant 0$. The discrete set of eigenvalues corresponding to positive integral values of $\tilde{\sigma}\frac{1}{2}(1+q^2)$ was found by Saffman & Taylor (1959) through

a power series truncation for each mode. When $q^2 < 0$, similar expressions for the eigenvectors can be constructed whenever $\mathrm{Re}\,\sigma > 0$, as shown in Tanveer (1987*b*) (Note $q^2 = -p^2$ in the notation of that paper), though this case will not be of interest here since we are interested in the stability of fingers for which (1.2) holds, where $\lambda < \frac{1}{2}$ and hence $q^2 > 0$.

Now, let us consider higher-order corrections f_1^{u} and g_1^{u} to the eigenmodes. It is convenient to define analytic functions in $|\zeta| < 1$ through the expressions

$$H_1(\zeta) = \frac{1}{2\pi}\int_0^{2\pi} \mathrm{d}\nu' \left[\frac{\mathrm{e}^{\mathrm{i}\nu'}+\zeta}{\mathrm{e}^{\mathrm{i}\nu'}-\zeta} + \frac{1+\mathrm{e}^{\mathrm{i}\nu'}\zeta}{1-\mathrm{e}^{\mathrm{i}\nu'}\zeta}\right] R_1(\nu'), \tag{3.19}$$

$$H_2(\zeta) = \frac{\mathrm{i}}{2\pi}\int_0^{2\pi} \mathrm{d}\nu' \left[\frac{\mathrm{e}^{\mathrm{i}\nu'}+\zeta}{\mathrm{e}^{\mathrm{i}\nu'}-\zeta} + \frac{1+\mathrm{e}^{\mathrm{i}\nu'}\zeta}{1-\mathrm{e}^{\mathrm{i}\nu'}\zeta}\right] R_2(\nu')2\sin\nu', \tag{3.20}$$

where $\mathrm{e}^{\sigma t}R_1(\nu)$ and $\mathrm{e}^{\sigma t}R_2(\nu)$ are the right-hand sides of (3.5) and (3.6), respectively, evaluated on $\zeta = \mathrm{e}^{\mathrm{i}\nu}$. Then using the same procedure as in the derivation of the differential equations (3.13) and (3.14), we find that for both symmetric and antisymmetric disturbances, without any loss of generality,

$$f_1^{\mathrm{u}} = \mathrm{e}^{\sigma t}H^{-1}(\zeta)\int_0^{\zeta} \mathrm{d}\zeta'\, H(\zeta')\left[H_{1_\zeta}(\zeta') - \frac{H_2(\zeta')}{\zeta'^2-1}\right]. \tag{3.21}$$

It is to be noted, however, that since f_0^{u} is different for symmetric and antisymmetric disturbances, $\mathrm{e}^{\sigma t}R_1$ and $\mathrm{e}^{\sigma t}R_2$, the right-hand sides of (3.5) and (3.6), are different. Thus, the expressions for H_1 and H_2 appearing in (3.21) will be different for symmetric and antisymmetric disturbances. It is not difficult to see that each of f_1^{u} and g_1^{u} is analytic everywhere on the semicircular arc except at $\zeta = \pm 1$. The assumed regular perturbation expansion (3.1) fails in the vicinity of $\zeta = \pm 1$, corresponding to the finger tails. There is need for an inner expansion near the tails; however, from prior experience with the steady state (Tanveer 1993), we do not expect that the inner–outer matching procedure will lead to any constraints on the eigenvalues, though we have not demonstrated this here. We will henceforth assume that there are no constraints on the eigenvalues σ arising from matching to a secondary asymptotic expansion near the tails.

(*b*) *Analytic continuation to* $|\zeta| > 1$ *and form of transcendental correction*

Now we turn our attention to trancendentally small terms in ϵ in $|\zeta| \leqslant 1$ in order to determine constraints on σ from the requirement that the eigenmodes when superposed on the steady state result in a smooth and analytic finger boundary. However, the coefficients of transcendentally small terms need not be calculated explicitly. Since the regular perturbation terms in (3.1) describe smooth fingers for any σ, the role of the transcendentally small terms that are normally subdominant is to cause the finger boundary to have singularities unless σ is constrained to special values. This is reflected in the non-uniqueness of analytic continuation across the arc of the unit ζ semicircle. By requiring that there is is an open neighbourhood of the finger boundary $|\zeta| = 1$, $\mathrm{Im}\,\zeta > 0$ where there is a unique analytic function f^{u} with asymptotic expansion (3.1), we rule out non-analytic finger boundaries and, in the process, determine the eigenvalues σ consistent with this requirement.

For the sake of algebraic simplicity, we find it more convenient to analytically continue the nonlinear evoluton equations (2.13) and (2.16) to $|\zeta| > 1$ and then linearize

PHILOSOPHICAL TRANSACTIONS OF THE ROYAL SOCIETY A MATHEMATICAL, PHYSICAL & ENGINEERING SCIENCES

the equations, rather than analytically continue the linear stability equations (2.31) and (2.32) directly. Following the same procedure used in the analytical continuation of the steady-state equations (Tanveer 1990), we find that these equations for $|\zeta| > 1$ are

$$\frac{2}{\pi}(f+g) = -\frac{\epsilon}{3\,Ca}\mathcal{I}[\kappa] - \frac{2\epsilon}{3\,Ca}\kappa, \tag{3.22}$$

$$\frac{2}{\pi}\zeta g_\zeta = -\frac{2\alpha}{\pi} + \mathcal{I}\left[-M + \mathrm{Re}[\zeta^* z_\zeta^* z_t(1-m)]\right] - 2M + \frac{2}{\pi}(1-m)\left[\frac{1}{\zeta}z_\zeta\left(\frac{1}{\zeta},t\right)f_t + \zeta z_\zeta f_t\left(\frac{1}{\zeta},t\right)\right], \tag{3.23}$$

where $\mathcal{I}$ is an integral operator defined below (see (3.26)) and $M = \mathrm{Re}[\zeta z_\zeta]m$, with m and κ as in (2.3) and (2.1), respectively. In these formulae, the following analytically continued expressions are used:

$$n_x = -\frac{1}{2}\frac{[\zeta z_\zeta + (1/\zeta)z_\zeta(1/\zeta,t)]}{z_\zeta^{1/2} z_\zeta^{1/2}(1/\zeta,t)}, \tag{3.24}$$

$$\bar{C} = -\frac{1}{z_\zeta^{1/2} z_\zeta^{1/2}(1/\zeta,t)}\left[1 + \zeta\frac{z_{\zeta\zeta}}{z_\zeta} + \frac{1}{\zeta}\frac{z_{\zeta\zeta}(1/\zeta,t)}{z_\zeta(1/\zeta,t)}\right]. \tag{3.25}$$

The integral operator $\mathcal{I}$, appearing in (3.22) and (3.23), is defined by

$$\mathcal{I}[g] = \frac{1}{2\pi \mathrm{i}}\int_C \frac{\mathrm{d}\zeta'}{\zeta'}\left[\frac{\zeta+\zeta'}{\zeta'-\zeta} + \frac{1+\zeta\zeta'}{1-\zeta\zeta'}\right] g(\zeta'). \tag{3.26}$$

Note that the operator $\mathcal{I}$ acts on an analytic function $g(\zeta)$ defined on the arc of the unit semicircle ($|\zeta| = 1$, $\mathrm{Im}\,\zeta > 0$) and produces a function analytic in $|\zeta| > 1$, where C denotes the contour coinciding with the arc of the upper half semicircle from $\zeta = 1$ at $\zeta = -1$.

Apart from a small neighbourhood around the critical point $\zeta = \mathrm{i}/q$, the form of the transcendental correction to the asymptotic series (3.1), though not the coefficients, can be deduced in the asymptotic limit of small Ca and ϵ with $\epsilon \ll Ca$ merely by linearizing (3.22) and (3.23) and assuming f and g to be small, each with an $\mathrm{e}^{\sigma t}$ time dependence. The set of homogeneous integro-differential equations associated with this linearization is further simplified, by using the Bretherton approximation (2.4)–(2.7) and neglecting the subdominant integral terms. As for the steady state (Tanveer 1990), the leading-order transcendental corrections for small $\mathcal{G}$ to (3.1) away from the critical point i/q are generally linear combinations of

$$\exp(\pm\mathcal{G}^{-1/2}[P + o(1)]), \tag{3.27}$$

where

$$P(\zeta) = \mathrm{e}^{\mathrm{i}3\pi/4}\int_{i/q}^{\zeta} \mathrm{d}\zeta \frac{(1+q^2\zeta^2)^{3/4}(\zeta^2+q^2)^{1/4}}{\zeta(\zeta^2-1)}. \tag{3.28}$$

The $o(1)$ terms appearing above depend on the eigenvalue σ that is assumed much smaller in size than $\mathcal{G}^{-1/2}$. Thus, the eigenvalues do not affect the Stokes sectors away from the critical point $\zeta = \mathrm{i}/q$. The Stokes sectors are bounded by Stokes lines, defined here as the lines where the two transcendental corrections of the form (3.27) exchange dominance. In this case, it is determined by the condition $\mathrm{Re}\,P = 0$, as

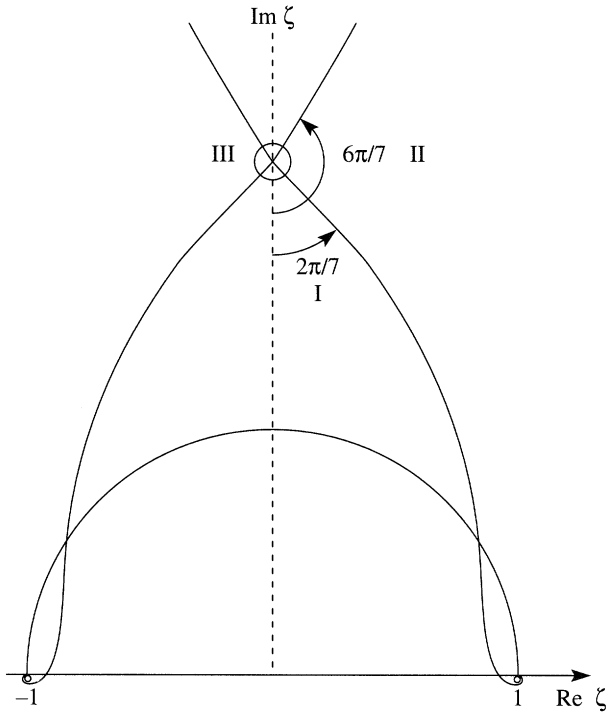

Figure 5. Stokes sectors intersecting the physical domain $|\zeta| \leqslant 1$ determined from $\operatorname{Re} P = 0$, with P given by (3.28).

shown in figure 5. This is the same as for the steady problem (Tanveer 1990) or even for the simpler MS boundary conditions (see Tanveer (1987*a*) for arguments leading to figure 5).

It is clear that if (3.1) is to be valid for a unique analytic function f^{u} in some neighbourhood of $|\zeta| = 1$, $\operatorname{Im}\zeta > 0$, then any trancendentally large correction to (3.1) of the form (3.27) has to be suppressed. Thus, in sector I that adjoins parts of the unit semicircular arc where $\operatorname{Re} P < 0$, transcendental correction to (3.1) of the form

$$\exp(-\mathcal{G}^{-1/2}[P + o(1)]) \tag{3.29}$$

has to be suppressed, while transcendental correction of the form

$$\exp(\mathcal{G}^{-1/2}[P + o(1)]) \tag{3.30}$$

has to be suppressed in sectors II and III. Each of the Stokes sectors I, II and III contains an anti-Stokes line emanating from $\zeta = \mathrm{i}/q$, where the ratio of the two exponentials in (3.27) is maximal or minimal in absolute value. Here, this is clearly determined by the condition $\operatorname{Im} P = 0$. Clearly, the imaginary ζ-axis between i and i/q is the anti-Stokes line in sector I, whereas anti-Stokes lines in sectors II and III approach $\zeta = \mathrm{i}/q$ symmetrically about the imaginary ζ-axis making a local angle of $\pm\frac{4}{7}\pi$, as is clear from a local expansion of (3.28). Since the coefficients of subdominant transcendental terms generally change across an anti-Stokes line (see for instance Berry (1991) and references therein), it is clear that in order to suppress transcendentally large terms in sectors I–III, it is enough to require that (3.1) hold on the three anti-Stokes lines away from an immediate neighbourhood of $\zeta = \mathrm{i}/q$.

(*c*) *Analysis in the inner regions and determination of spectrum*

As $\zeta = \mathrm{i}/q$ is approached, then, as discussed in connection to earlier steady-state analysis (Tanveer 1990), the form of the transcendental correction (3.27) is altered first in a neighbourhood of $\zeta = \mathrm{i}/q$ where χ_3, as defined in (3.31), is $O(1)$. In this neighbourhood, the asymptotic relation (3.1) still remains valid except when $|\chi_3| = O(\tilde{\beta}_4^{6/7}) \ll 1$, where $\tilde{\beta}_4$ is defined in (3.34). χ_3 is defined by the relation

$$1 + \mathrm{i}q\zeta = r_1 \tilde{\beta}_1^{12/7} \tilde{\beta}_4^{-6/7} \chi_3, \tag{3.31}$$

where

$$r_1 = 2^{-3/2}(1.3375)^{3/4}\, Ca^{1/2}\, \frac{(1-q^4)}{q^2}, \tag{3.32}$$

$$\tilde{\beta}_1 = \tfrac{1}{3}\pi 2^{3/2}(3.878)(1.3375)^{-7/4} \frac{\epsilon q^2}{Ca^{3/2}(1+q^2)(1-q^2)^2}, \tag{3.33}$$

$$\tilde{\beta}_4 = \tfrac{1}{3}2^{-1/4}\pi^5(1.3375)^{-21/8} \frac{\epsilon^2 q^4}{Ca^{11/4}(1+q^2)^2(1-q^2)^4}. \tag{3.34}$$

It is to be realized that when the steady-state relation (1.2) holds, $r_1 \ll 1$, $\tilde{\beta}_1 = O(1)$ and, from (3.34), $\tilde{\beta}_4 = O(Ca^{1/4}\,\tilde{\beta}_1^2) \ll 1$. Further, it can be seen from (1.2), (2.28), (3.32)–(3.34) that when $\chi_3 = O(1)$, $|1 + \mathrm{i}q\zeta| \ll 1$. For $\chi_3 = O(1)$ but much greater than $\tilde{\beta}_4^{6/7}$, as discussed in the context of steady state (Tanveer 1990), the form of the transcendental corrections for small $\tilde{\beta}_4$ become (equations (5.54) and (5.55) of Tanveer (1990))

$$\hat{F}_{H_1} = \exp\left[\tfrac{1}{6}\tilde{\beta}_1^3\tilde{\beta}_4^{-2}\left(\int_0^{\chi_3} \mathrm{d}\chi_3\{\chi_3^{1/6} - (\chi_3^{1/3} + 36\chi_3^{3/2})^{1/2} + o(1)\}\right)\right], \tag{3.35}$$

$$\hat{F}_{H_2} = \exp\left[\tfrac{1}{6}\tilde{\beta}_1^3\tilde{\beta}_4^{-2}\left(\int_0^{\chi_3} \mathrm{d}\chi_3\{\chi_3^{1/6} + (\chi_3^{1/3} + 36\chi_3^{3/2})^{1/2} + o(1)\}\right)\right]. \tag{3.36}$$

Clearly, for $|\chi_3| \gg 1$, $\hat{F}_{H_1}$ matches with $\exp\{\mathcal{G}^{-1/2}[P + o(1)]\}$, while $\hat{F}_{H_2}$ matches with $\exp\{-\mathcal{G}^{-1/2}[P + o(1)]\}$ as $\zeta \to \mathrm{i}/q$. Notice that for $\chi_3 = O(1)$ the anti-Stokes lines determined from requiring $\hat{F}_{H_1}/\hat{F}_{H_2}$, or its reciprocal to be maximal, is now determined by

$$\mathrm{Im}\left[\int_0^{\chi_3} \mathrm{d}\chi_3\,(\chi_3^{1/3} + 36\chi_3^{3/2})^{1/2}\right] = 0. \tag{3.37}$$

For large $|\chi_3|$, the anti-Stokes lines of interest to us (in the sense that they lie inside sectors I–III in figure 5) are asymptotically given by $\arg\chi_3 = 0, \pm\frac{4}{7}\pi$, as expected. For $|\chi_3| \ll 1$, these anti-Stokes lines approach $\arg\chi_3 = 0, \pm\frac{6}{7}\pi$, as is clear from a local expansion of (3.37). To avoid transcendentally large corrections of the form (3.29) in sector I, it is necessary that an asymptotic correction of the form $\hat{F}_{H_2}$ is absent on the positive χ_3-axis. Similarly, in order to avoid transcendentally large contributions of the type (3.30) in sectors II and III, it is enough to suppress transcendentally large terms of the type $\hat{F}_{H_1}$ along anti-Stokes lines that asymptotically approach $\arg\chi_3 = \pm\frac{6}{7}\pi$ as $\chi_3 \to 0$. However, to determine if this is possible, it is necessary to go even closer to $\zeta = \mathrm{i}/q$, where the asymptotic expansion (3.1), as well as the form of the transcendental corrections (3.35), (3.36) for small $\tilde{\beta}_4$, becomes invalid.

As for the steady state, we introduce local inner variables near $\zeta = \mathrm{i}/q$:

$$1 + \mathrm{i}q\zeta = r_1\chi, \tag{3.38}$$

$$f = -\frac{2q^2}{1+q^2} r_1^2 \tilde{F}(\chi, t), \tag{3.39}$$

$$g = -\frac{2q^2}{1+q^2} r_1^2 \tilde{\omega}(\chi, t). \tag{3.40}$$

Then to the leading order, (3.22) and (3.23) reduce to

$$-\tilde{F} - \tilde{\omega} = \tilde{\beta}_1 (\chi - \tilde{F}_\chi)^{-1/3} (1 - \alpha_4 \tilde{F}_t)^{2/3} + \tilde{\beta}_4 (1 - \tilde{F}_{\chi\chi}) (\chi - \tilde{F}_\chi)^{-3/2}, \tag{3.41}$$

$$\tilde{\omega}_\chi = (\chi - \tilde{F}_\chi)^{-1/3} (1 - \alpha_4 \tilde{F}_t)^{2/3} - \tilde{\beta}_3 (\chi - \tilde{F}_\chi)^{-11/6} (1 - \alpha_4 \tilde{F}_t)^{2/3} (1 - \tilde{F}_{\chi\chi}) + \tilde{\beta}_6 \tilde{F}_t, \tag{3.42}$$

where

$$\tilde{\beta}_3 = \pi^2 2^{-9/4} (1.3375)^{-9/8} \frac{\epsilon q^2}{Ca^{3/4} (1+q^2)(1-q^2)^2}, \tag{3.43}$$

$$\alpha_4 = \frac{4}{\pi} \frac{q^2}{1+q^2} r_1^2, \tag{3.44}$$

$$\tilde{\beta}_6 = \frac{2}{\pi} (1 - q^2) r_1. \tag{3.45}$$

Between the two equations (3.41) and (3.42), $\tilde{\omega}$ can be eliminated. Further, if we decompose

$$\tilde{F}(\chi, t) = F(\chi) + \mathrm{e}^{\sigma t} F^{\mathrm{u}}(\chi), \tag{3.46}$$

where F is the steady and F^{u} the unsteady part, then F satisfies the following steady-state equation (equation (5.41) of Tanveer (1990), though with somewhat differing notation):

$$\begin{aligned} &F' + (\chi - F')^{-1/3} - \tilde{\beta}_3 (1 - F'') (\chi - F')^{-11/6} - \tfrac{1}{3} \tilde{\beta}_1 (\chi - F')^{-4/3} (1 - F'') \\ &-\tilde{\beta}_4 \{ F''' (\chi - F')^{-3/2} + \frac{3}{2} (\chi - F')^{-5/2} (1 - F'')^2 \} = 0, \end{aligned} \tag{3.47}$$

while the linearized stability equation for F^{u} is given by

$$\begin{aligned} &[\tilde{\beta}_6 - \tfrac{2}{3} \alpha_4 (\chi - F')^{-1/3} + \tfrac{1}{2} \alpha_4 \tilde{\beta}_3 (\chi - F')^{-11/6} (1 - F'') \\ &+ \tfrac{2}{9} \tilde{\beta}_1 \alpha_4 (\chi - F')^{-4/3} (1 - F'')] \sigma F^{\mathrm{u}} - \tfrac{2}{3} \tilde{\beta}_1 \alpha_4 (\chi - F')^{-1/3} \sigma F^{\mathrm{u}}_\chi \\ &+ [1 + \tfrac{1}{3} (\chi - F')^{-4/3} - \tfrac{11}{6} \tilde{\beta}_3 (\chi - F')^{-17/6} (1 - F'') - \tfrac{4}{9} \tilde{\beta}_1 (\chi - F')^{-7/3} (1 - F'') \\ &- \tfrac{3}{2} \tilde{\beta}_4 F''' (\chi - F')^{-5/2} - \tfrac{15}{4} \tilde{\beta}_4 (1 - F'')^2 (\chi - F')^{-7/2}] F^{\mathrm{u}}_\chi \\ &+ [\tfrac{1}{3} \tilde{\beta}_1 (\chi - F')^{-4/3} + 3 \tilde{\beta}_4 (1 - F'') (\chi - F')^{-5/2} + \tilde{\beta}_3 (\chi - F')^{-11/6}] F^{\mathrm{u}}_{\chi\chi} \\ &- \tilde{\beta}_4 (\chi - F')^{-3/22} F^{\mathrm{u}}_{\chi\chi\chi} = 0. \end{aligned} \tag{3.48}$$

Since, from definition of the parameters, $\tilde{\beta}_3 = O(Ca^{3/4}\, \tilde{\beta}_1)$, $\tilde{\beta}_4 = O(Ca^{1/4}\, \tilde{\beta}_1^2)$. Thus, when $\tilde{\beta}_1 = O(1)$, as is the case when (1.2) holds, then $\tilde{\beta}_3 \ll \tilde{\beta}_4 \ll \tilde{\beta}_1$. Here, we only consider the stability of the first few branches of steady solutions for which $1/\tilde{\beta}_1 = O(1)$. Since $\tilde{\beta}_4$ and $\tilde{\beta}_3$ are each small compared to unity, we assume that

$$F^{\mathrm{u}} \sim \hat{F}^0, \tag{3.49}$$

where $\hat{F}^0$ satisfies

$$\hat{\sigma} \hat{F}^0 + [1 + \tfrac{1}{3} (\chi - F^{0'})^{-4/3} - \tfrac{4}{9} \tilde{\beta}_1 (\chi - F^{0'})^{-7/3} (1 - F^{0''})] \hat{F}_\chi + \tfrac{1}{3} \tilde{\beta}_1 (\chi - F^{0'})^{-4/3} \hat{F}_{\chi\chi} = 0, \tag{3.50}$$

PHILOSOPHICAL TRANSACTIONS OF THE ROYAL SOCIETY A MATHEMATICAL, PHYSICAL & ENGINEERING SCIENCES

where

$$\hat{\sigma} = \tilde{\beta}_6 \sigma, \tag{3.51}$$

and F^0 is the corresponding steady-state function satisfying the following (equation (5.71) of Tanveer (1990)) equation:

$$F^{0'} + (\chi - F^{0'})^{-1/3} - \tfrac{1}{3}\tilde{\beta}_1(\chi - F^{0'})^{-4/3}(1 - F^{0''}) = 0. \tag{3.52}$$

For large $|\chi|$, we seek a unique solution $\hat{F}^0$ to satisfy the asymptotic condition

$$\hat{F}^0 \sim C\mathrm{e}^{-\hat{\sigma}\chi} \tag{3.53}$$

for $\arg\chi$ in $[-\frac{6}{7}\pi, \frac{6}{7}\pi]$, where C is some normalization constant. The behaviour (3.53), with appropriate choice of C, matches with (3.15) or (3.16) when $|1 + \mathrm{i}q\zeta| \to 0$. We notice that (3.50) also allows an asymptotic solution for large $|\chi|$ of the form

$$F_{H_1} = \exp\left(-\frac{9}{7\hat{\beta}_1}\chi^{7/3}[1 + o(1)]\right). \tag{3.54}$$

This matches with $\hat{F}_{H_1}$, given in (3.35), as $|\chi_3| \to 0$. To the extent that (3.49) is valid, by requiring $\hat{F}^0$ to satisfy (3.53) for large $|\chi|$ when $\arg\chi$ is in $[-\frac{6}{7}\pi, \frac{6}{7}\pi]$, we suppress transcendentally large corrections of the form (3.54) for $\arg\chi = \pm\frac{6}{7}\pi$ and hence suppress the transcendentally large contribution $\hat{F}_{H_1}(\chi_3)$, implying in turn that transcendentally large contributions in $\mathcal{G}$ in the form (3.30) is absent in sectors II and III (figure 5). Transcendentally large corrections for small $\tilde{\beta}_4$ of the form $\hat{F}_{H_2}(\chi_3)$ on the postive real χ_3-axis, and therefore a contribution of type (3.29) in sector I, is ruled out by approximation (3.49), since (3.50) allows no transcendental correction to (3.53) that can be matched to $\hat{F}_{H_2}$ as $\chi_3 \to 0$. Terms matching such exponentials are generally present in solutions to (3.48) but are suppressed when (3.49) is valid.

Thus, if (3.49) is valid (a question to be taken up later), then the construction of a unique solution to (3.52) that satisfies the asymptotic boundary condition (3.53) for $\arg\chi$ in $[-\frac{6}{7}, \frac{6}{7}\pi]$ guarantees that (3.1) is valid in sectors I–III as required. Given that for large $|\chi|$, $\arg\chi = \pm\frac{3}{7}\pi$ is an anti-Stokes line†, it follows that satisfaction of asymptotic condition (3.53) on these lines guarantees the absence of transcendental corrections of the form (3.54) for $0 \leqslant |\arg\chi| < \frac{6}{7}\pi$. In passing, we remark that transcendental terms of the form (3.54) born at $|\arg\chi| = \frac{6}{7}\pi$ remain subdominant to (3.53) until the Stokes lines at $|\arg\chi| = \frac{15}{14}\pi$.

We now describe the numerical procedure used to determine conditions on σ that guarantee that a unique solution $\hat{F}^0$ to (3.50) exists that satisfies (3.53) for large $|\chi|$ when $\arg\chi = \pm\frac{3}{7}\pi$. First, in order to obtain acceptable errors in the numerical integration of (3.50), we calculated higher order corrections to the asymptotic behaviour (3.53) for large χ to obtain

$$\begin{aligned}\hat{F}^0 \sim C\exp[&-\hat{\sigma}\chi + \hat{\sigma}(-1 + \tilde{\beta}_1\hat{\sigma})\chi^{-1/3} + \tfrac{1}{3}\tilde{\beta}_1\hat{\sigma}\chi^{-4/3} + \tfrac{1}{15}\hat{\sigma}(5 - 7\tilde{\beta}_1\hat{\sigma} + 2\hat{\beta}_1^2\hat{\sigma}^2)\chi^{-5/3} \\ &+ \tfrac{1}{18}\hat{\sigma}(-12\tilde{\beta}_1\hat{\sigma} + 5\tilde{\beta}_1^2\hat{\sigma})\chi^{-8/3} + \tfrac{1}{81}\hat{\sigma}(-27 + 48\tilde{\beta}_1\hat{\sigma} - 26\tilde{\beta}_1^2\hat{\sigma}^2 + 5\tilde{\beta}_1^3\hat{\sigma}^3)\chi^{-3}].\end{aligned} \tag{3.55}$$

† This anti-Stokes line is concerned with the reduced equation (3.50) rather than (3.48) and is defined by the maximal or minimal ratio of the size of the transcendental term F_{H_1} in (3.54) to that of the algebraic terms in (3.53) for large $|\chi|$.

This is obtained through a routine dominant balance procedure applied to (3.50) and using the asymptotic relation

$$F^{0'} \sim \chi^{-1/3} + \tfrac{1}{3}\tilde{\beta}_1\chi^{-4/3} + \tfrac{1}{3}\chi^{-5/3} + \tfrac{1}{9}\tilde{\beta}_1\chi^{-8/3} - \tfrac{1}{3}\chi^{-3} + \tfrac{1}{27}\tilde{\beta}_1^2\chi^{-11/3} + \tfrac{2}{27}\tilde{\beta}_1\chi^{-4} \quad (3.56)$$

for the steady state. Equation (3.55) is used to calculate $\hat{F}^0$ and $\hat{F}^{0'}$ at $\chi = \bar{L}e^{\pm i3\pi/7}$. Each of these points is used as an initial point for integrating (3.50) along a straight line towards $\chi = 0$, using the computed steady-state solution $F^{0'}$, where the normalization constant C is chosen so that $\hat{F}^0(0) = 1$ on either paths. By choosing $\bar{L}$ to be a suitably large positive number, this numerical procedure rules out a behaviour like (3.54) for large $|\chi|$ for $\arg\chi = \pm\frac{3}{7}\pi$. We denote the solution on the two paths by $\hat{F}^{0^+}$ and $\hat{F}^{0^-}$. Generally, for arbitrary $\hat{\sigma}$, our numerical calculations show that

$$R = \hat{F}^{0^+}_{\chi}(0) - \hat{F}^{0^-}_{\chi}(0) \neq 0. \quad (3.57)$$

On examination of the analytic continuation of (3.5) and (3.6), it follows that the coefficients of the linear equation for f^{u} (which depends on the prior computed steady-state function f^{s}) can have no singularity in $|\zeta| > 1$ closer to the arc of the unit circle $|\zeta| = 1$ than those for $|1 + \mathrm{i}q\zeta| = O(r_1)$. In this neighbourhood, i.e. when $\chi = O(1)$, details of of the steady-state function $F^{0'}$ discussed later reveal no singularity for $\mathrm{Re}\,\chi \geqslant 0$. Thus, any solution $\hat{F}^0$ satisfying the linear equation (3.50) can have no singularity in this part of the χ plane. Also, when $R \neq 0$, the computed functions $\hat{F}^{0^+}$ and $\hat{F}^{0^-}$ cannot be analytic continuations of each other. This can only be consistent with a branch point singularity of the the eigenfunction $f^{\mathrm{u}}(\zeta, t)$ on $|\zeta| = 1$, corresponding to a non-analytic finger boundary.

Thus, the requirement $R = 0$ is forced upon us when we require the eigenmodes to preserve the analyticity of the finger boundary. Indeed, $R = 0$ is also sufficient to guarantee analyticity of the finger boundary as we now argue. Note that (3.50) is a second-order differential equation. Prior steady-state computations showed no singularity of $(\chi - F^{0'})^{-4/3}$ (and therefore of the coefficients of the linear differential equation (3.50) for $\hat{F}^0$) for $\mathrm{Re}\,\chi > 0$. Thus, the continuity of $\hat{F}^0$ and its first derivative at $\chi = 0$, implied by $R = 0$, guarantees that $\hat{F}^{0^+}$ and $\hat{F}^{0^-}$ are analytic continuations of each other across the positive $\mathrm{Re}\,\chi$-axis and therefore in the entire right half χ plane. Since the singularities of the steady state functions $(\chi - F^{0'})^{-4/3}$, occurring in (3.50), cannot be located anywhere where $\mathrm{Re}\,\chi > 0$ and $|\chi| \gg 1$ (where (3.56) applies), it means that the closest singularities to the upper-half ζ semicircle must be when $|\chi| = O(1)$ with $\mathrm{Re}\,\chi < 0$. It follows that by requiring $R = 0$ in the procedure described in the last paragraph, we have a sufficient condition for the finger boundary to be analytic. We now turn to numerically determining $\hat{\sigma}$ and hence the spectrum of the linear stability operator by requiring

$$R(\hat{\sigma}) = 0. \quad (3.58)$$

We assume $R(\hat{\sigma})$ to be a locally analytic function of $\hat{\sigma}$; this is consistent with numerical calculations that showed that the integral of $R(\hat{\sigma})$ over some arbitrarily chosen closed contour in the $\hat{\sigma}$ plane is zero to within numerical accuracy of the quadrature. It is convenient to monitor numerically calculated

$$\mathcal{N} = \frac{1}{2\pi\mathrm{i}} \oint_C \mathrm{d}\hat{\sigma} \frac{R'(\hat{\sigma})}{R(\hat{\sigma})} \quad (3.59)$$

on closed contours C in the complex $\hat{\sigma}$ plane to locate zeros of R. For the first

branch of steady state for which $3/\hat{\beta}_1 = 9.843\,454\,86$, i.e. $k = 2.832$ in relation (1.2), we searched for a zero of $R(\hat{\sigma})$ extensively in the complex right half $\hat{\sigma}$ plane, but were unable to find any. Since the coefficients of each derivative of $\hat{F}$ are real for positive χ, it is clear that eigenvalues, if complex, occur in conjugate pairs. Our search also included looking for change of sign in $R(\hat{\sigma})$ by marching along the real positive $\hat{\sigma}$-axis upto $\hat{\sigma} = 8$. We evaluated $\mathcal{N}$ for various C, chosen in the entire $0 \leqslant \mathrm{Re}\,\hat{\sigma} \leqslant 6$, $0 \leqslant \mathrm{Im}\,\hat{\sigma} \leqslant 6$, with the exception of a small box $0 \leqslant \mathrm{Re}\,\hat{\sigma} \leqslant 0.05$, $0 \leqslant \mathrm{Im}\,\hat{\sigma} \leqslant 0.05$, that could not be investigated because of integration accuracy. We noticed that a large contour C for the calculation in (3.59) led to numerical inaccuracies due to additive cancellation of large integrands. So we divided the whole region up into smaller rectangles, and each time we found the answer to (3.59) to be zero, within reasonable accuracy. We also monitored

$$\frac{1}{2\pi \mathrm{i}} \oint_C \mathrm{d}\hat{\sigma} \frac{\hat{\sigma} R'(\hat{\sigma})}{R(\hat{\sigma})} \tag{3.60}$$

at the same time and found it to be zero within the accuracy of the integration procedure. We also used Newton iteration to seek the possibility that there may be eigenvalues in the small box $0 \leqslant \mathrm{Im}\,\hat{\sigma} \leqslant 0.05$, $0 \leqslant \mathrm{Re}\,\hat{\sigma} \leqslant 0.05$. Each time there was convergence to some value for $\hat{\sigma}$, we found that this value shifted to even smaller value as the number of integration points was increased. This led us to conclude that the eigenvalue of the discretized numerical system actually corresponds to the zero eigenvalue, corresponding to a pure translation mode. Based on evidence from our numerical search, we conclude that there are no unstable eigenvalues for this branch of solution, which corresponds to the smallest finger width λ.

For the second branch, corresponding to $3/\tilde{\beta}_1 = 16.795\,856$, a Newton iterative procedure gave us the value

$$\hat{\sigma} = 3.750, \tag{3.61}$$

which was consistent with a value of $\mathcal{N} = 1$ for a contour C chosen around this point in the complex $\hat{\sigma}$ plane. Computation for other branches of steady-state solution also resulted in unstable eigenvalues. We conclude that, in the asymptotic limit $\epsilon \ll Ca \ll 1$, only one branch of steady-state solution, the one for which k in relation (1.2) is the smallest ($k = 2.832$), is stable where as other branches are unstable.

Despite obtaining the results on spectrum as given previously, which is the main objective of our stability analysis, we must check for consistency of our assumption (3.49), since for small $\tilde{\beta}_4$, (3.48) also allows an asymptotic solution of the form

$$F_{H_2} = \exp\left[\frac{\tilde{\beta}_1}{3\tilde{\beta}_4} \int_0^{\chi} [\chi - F^{0'}]^{1/6}[1 + o(1)]\right]. \tag{3.62}$$

This contribution can dominate $\hat{F}^0$ in certain sectors of the complex χ-plane. Note that for large χ, (3.62) reduces to

$$F_{H_2} \sim \exp\left[\frac{2\tilde{\beta}_1}{7\tilde{\beta}_4} \chi^{7/6}(1 + o(1))\right], \tag{3.63}$$

which is transcendentally large for large χ on the positive χ-axis. Thus, the matching condition (3.49) cannot hold if transcendental corrections of the form (3.62) are not suppressed appropriately. The rest of this section will be devoted to demonstrating that this can be done without any additional constraints on σ.

The behaviour of the unsteady function F^{u} (3.48) is clearly related to the behaviour of the steady-state function F satisfying (3.47). We first need to examine F in greater detail than reported earlier (Tanveer 1990). The two-term formal asymptotic expansion for F' for small $\tilde{\beta}_3 \ll \tilde{\beta}_4 \ll 1$ can be written as

$$F' \sim F^{0'} + F^{1'}, \tag{3.64}$$

where F^0 satisfies (3.52), while F^1 satisfies

$$F^{1'}\{1 + \tfrac{1}{3}(\chi - F^{0'})^{-4/3} - \tfrac{4}{9}\tilde{\beta}_1(\chi - F^{0'})^{-7/3}(1 - F^{0''})\} + \tfrac{1}{3}\tilde{\beta}_1(\chi - F^{0'})^{-4/3}F^{1''}$$
$$= 2\tilde{\beta}_4 \frac{\mathrm{d}^2}{\mathrm{d}\chi^2}(\chi - F^{0'})^{-1/2}. \tag{3.65}$$

The asymptotic boundary condition for $F^{1'}$ for large χ with $\arg\chi = \frac{3}{7}\pi$, which is consistent with (3.56), is given by

$$F^{1'} \sim -3\tilde{\beta}_4/2\chi^{5/2}. \tag{3.66}$$

An explicit expression for $F^{1'}$ is possible. If we define

$$F_{\mathrm{H}}(\chi) = \exp\left\{ -\frac{3}{\tilde{\beta}_1}\int_0^{\chi} \mathrm{d}\chi[(\chi - F^{0'})^{4/3} + \tfrac{1}{3} - \tfrac{4}{9}\tilde{\beta}_1(\chi - F^{0'})^{-1}(1 - F^{0''})]\right\}, \tag{3.67}$$

then

$$F^{1'} = F_{\mathrm{H}}(\chi)\int_{\infty \mathrm{e}^{\mathrm{i}3\pi/7}}^{\chi} \mathrm{d}\chi' \frac{6\tilde{\beta}_4}{\tilde{\beta}_1}\frac{(\chi' - F^{0'}(\chi'))^{4/3}}{F_{\mathrm{H}}(\chi')}\frac{\mathrm{d}^2}{\mathrm{d}\chi'^2}(\chi' - F^{0'}(\chi'))^{-1/2}. \tag{3.68}$$

In order for (3.64) to hold it is necessary that transcendental corrections to (3.64) for small $\tilde{\beta}_4$ of the form (3.62) are suppressed when they are large. However, to determine if this is possible, it is necessary to investigate the inner neighbourhood of the points in the χ-plane where the regular perturbation expansion (3.64) breaks down. It is clear from (3.52) that if $\chi = \chi_{\mathrm{p}}$ that the singularities of $F^{0'}$ in the form $(\chi - \chi_{\mathrm{p}})^{-3/4}$ are admitted. In order to determine the location of one or more χ_{p} for $\mathrm{Im}\,\chi_{\mathrm{p}} \geqslant 0$, we carried out the following numerical procedure.

We numerically integrate (3.52), with asymptotic boundary condition (3.56) used to find the initial conditions on $F^{0'}$ and $F^{0''}$ at $\bar{L}\mathrm{e}^{\mathrm{i}3\pi/7}$ for large positive $\bar{L}$. ($\bar{L} = 20$ appeared to be sufficient for our purposes). In order to avoid numerically awkward implementation of the requirement that $\arg(\chi - F^{0'})$ changes continously along the integration path, it was convenient to introduce $g(\chi) = (\chi - F^{0'})^{-1/3}$ as the dependent variable. The equation for g, easily derived from (3.52), does not contain any fractional power. The initial condition for g is computed from (3.56) by taking the principal branch in the transformation from $F^{0'}$ to g. Integration proceeded along a straightline towards $\chi = 0$ in the same manner, similar to that described in Tanveer (1990). Recall that an auxiliary Newton iterative procedure to ensure $\mathrm{Im}\,F^{0'}(0) = 0$ can be used to determine $\tilde{\beta}_1$ or equivalently determine the selected finger width λ. With the selected value of $\tilde{\beta}_1$, and corresponding $g(0)$ (and therefore $F^{0'}(0)$), we proceed to numerically integrate g along small closed paths C in the complex χ-plane for $\mathrm{Im}\,\chi \geqslant 0$. We examine if the function g returns to the same value and $\oint_C \mathrm{d}\chi g'/g$ is zero. When this is the case, we conclude that the function $g(\chi)$ has no zeros or singularities within that contour (note that the equation for g does not admit poles). When this was not the case for a sufficiently small contour, we monitored if $g(\chi)$

returned to the same value and if $1/(2\pi\mathrm{i})\oint_C \mathrm{d}\chi\, g'/g$ was equal to a multiple of 1 (to within numerical accuracy) when we traversed the closed contour C four times. When this was the case, $1/(2\pi\mathrm{i})\oint_C \mathrm{d}\chi\,\chi g'/g$ provides us with the location of χ_p, which was found to be consistent with the physical location of the contour C. No singularities were found for $\mathrm{Re}\,\chi > 0$, despite an exhaustive search. Our calculations gave us one singularity at χ_p for $\mathrm{Im}\,\chi \geqslant 0$ for $\mathrm{Re}\,\chi < 0$. For the first branch of the solution, we found $\chi_\mathrm{p} = -1.933\,387 + \mathrm{i}0.989\,171\,4$. Since symmetry condition $\mathrm{Im}\,g(\chi) = 0$, and therefore $\mathrm{Im}\,F^{0'}(\chi) = 0$ is found to be satisfied on the postive real χ-axis as part of determining $\tilde{\beta}_1$ (Tanveer 1990), it follows that there must also be a singularity of $F^{0'}$ at χ_p^*. χ_p and χ_p^* were determined to be the singularities closest to the imaginary axis and therefore most relevant to determining coefficients of transcendental correction (3.62) on the real positive χ-axis.

At $\chi = \chi_\mathrm{p}$, the numerically observed behaviour is consistent with

$$-F^{0'} \sim \mathrm{e}^{\mathrm{i}3\pi/2}\tilde{\beta}_1^{3/4}4^{-3/4}(\chi-\chi_\mathrm{p})^{-3/4}, \tag{3.69}$$

which can be deduced as a possible behaviour of $F^{0'}$ directly from (3.52). From (3.67), it follows on integration that, near $\chi = \chi_\mathrm{p}$,

$$F^{1'} \sim a_{11}(\chi-\chi_\mathrm{p})^{-7/4} - \mathrm{e}^{-\mathrm{i}3\pi/4}\tfrac{15}{8}\tilde{\beta}_4(\tfrac{1}{4}\tilde{\beta}_1)^{5/8}(\chi-\chi_\mathrm{p})^{-13/8}, \tag{3.70}$$

where

$$a_{11} = \tilde{a}_{11}\int_{\infty\mathrm{e}^{\mathrm{i}3\pi/7}}^{\chi_\mathrm{p}} \mathrm{d}\chi' \frac{6\tilde{\beta}_4}{\tilde{\beta}_1}\frac{(\chi'-F^{0'}(\chi'))^{4/3}}{F_\mathrm{H}(\chi')}\frac{\mathrm{d}^2}{\mathrm{d}\chi'^2}(\chi'-F^{0'}(\chi'))^{-1/2}, \tag{3.71}$$

where

$$\tilde{a}_{11} = \lim_{\chi\to\chi_\mathrm{p}}(\chi-\chi_\mathrm{p})^{7/4}F_\mathrm{H}(\chi). \tag{3.72}$$

Near $\chi = \chi_\mathrm{p}$, we introduce the inner variables

$$\chi - \chi_\mathrm{p} - s = \mathrm{e}^{-\mathrm{i}2\pi/7}\tilde{\beta}_1^{-9/7}\tilde{\beta}_4^{8/7}\xi, \tag{3.73}$$

where $s \ll 1$ is a constant that will be conveniently chosen later, and

$$-F' = \mathrm{e}^{\mathrm{i}12\pi/7}\tilde{\beta}_1^{12/7}\tilde{\beta}_4^{-6/7}G'(\xi). \tag{3.74}$$

Then, to the leading order, the steady-state equation (3.47) reduces to

$$-G' - \tfrac{1}{3}G'^{-4/3}G'' + G'''G'^{-3/2} - \tfrac{3}{2}G''^2G'^{-5/2} = 0. \tag{3.75}$$

For large ξ, a dominant balance procedure applied to (3.75) shows that a possible behaviour of G is given by

$$G' \sim [\tfrac{1}{4}]^{3/4}\xi^{-3/4} + \frac{45}{2^{13/4}}\xi^{-13/8} + a_1\xi^{-7/4} + \tfrac{225}{2}\xi^{-5/2} + \cdots, \tag{3.76}$$

where a_1 is arbitrary at this point. This arbitrariness is not unexpected since (3.75) is an autonomous equation and a shift in ξ is reflected in (3.76) by a change in a_1. By choosing

$$s = -\tilde{\beta}_4\tilde{\beta}_1^{-3/4}4^{3/4}\mathrm{e}^{-i3\pi/2}\tfrac{4}{3}a_{11}, \tag{3.77}$$

the first three terms of (3.76) can be matched with the most singular terms of $F^{0'} + F^{1'}$ (shown in (3.69) and (3.70)) as $\chi \to \chi_\mathrm{p}$, provided $a_1 = 0$ in (3.76). To match with the $\xi^{-5/2}$ term in (3.76), we need to consider the $O(\tilde{\beta}_4^2)$ term in the outer

asymptotic expansion (3.64), which is not included in this analysis. However, (3.75) also allows transcendental correction to the asymptotic behaviour (3.76). Its form can be deduced by linearizing (3.75) about (3.76) and looking for WKB-type solutions for large $|\xi|$ to the associated homogeneous equation. Transcendental correction to (3.76) is found to be

$$\mathrm{e}^{(1/4)^{1/8}(8/21)\xi^{7/8}[1+o(1)]}. \tag{3.78}$$

This is transcendentally large, in particular for large positive ξ on the real axis. Solutions to (3.75) that do not contain terms of the type (3.78) for large positive real ξ can be obtained by using (3.76) (with $a_1 = 0$) to determine initial condition on G' and G'' at a faraway point and integrating (3.75) towards $\xi = 0$. Note that the transcendental term (3.78) matches with the transcendental correction (3.62) as $\chi \to \chi_{\mathrm{p}}$. Thus, if transcendental large correction (3.78) is avoided on the positive ξ-axis for large $|\xi|$, it ensures the absence of a transcendental correction of the form (3.62) on the anti-Stokes line determined from

$$\mathrm{Im} \int_{\chi_{\mathrm{p}}}^{\chi} \mathrm{d}\chi \, (\chi - F^{0'}(\chi))^{1/6}(1 + o(1)) = 0 \tag{3.79}$$

with $\arg(\chi - \chi_{\mathrm{p}}) \to -\frac{2}{7}\pi$ as $\chi \to \chi_{\mathrm{p}}$ (i.e. $\arg \xi = 0$). This anti-Stokes line has been computed in figure 6 and is seen to approach the positive real χ-axis for large χ. Adjacent anti-Stokes lines which start at $\chi = \chi_{\mathrm{p}}$ with $\arg(\chi - \chi_{\mathrm{p}}) = \frac{6}{7}\pi$ and $\frac{10}{7}\pi$ are found to completely remain in the region $\mathrm{Re}\,\chi < 0$ and asymptote towards $\arg \chi = \pm\frac{6}{7}\pi$ as $|\chi| \to \infty$. Thus, in effect, by ruling out transcendentally large terms of the form (3.78) for large positive ξ, we eliminate transcendentally large correction for large χ of the form (3.62) in the relevant regions of the complex χ-plane where (3.64) is assumed to hold. Given that $F^{0'}$ is real on the positive real χ-axis, from symmetry, similar inner–outer matching follows in a neighbourhood of the singular point $\chi = \chi_{\mathrm{p}}^*$.

Now, we turn to the singularities of the eigenmode function $\hat{F}^0$ satisfying (3.50) with a view to determining where (3.49) breaks down and how transcendental terms of the form (3.62) can be avoided. Given the similarity of (3.50) and (3.65), it is not difficult to deduce that at $\chi = \chi_{\mathrm{p}}$, $\hat{F}^0_\chi$ is singular such that as $\chi \to \chi_{\mathrm{p}}$,

$$\hat{F}^0_\chi \sim D(\chi - \chi_{\mathrm{p}})^{-7/4}, \tag{3.80}$$

where D is some non-zero constant, the actual value of which is unimportant since (3.50) is a linear homogeneous equation. By using transformations (3.73) and (3.74), (3.48) reduces to

$$\begin{aligned}\mathrm{e}^{-\mathrm{i}2\pi/7}\hat{\sigma}\tilde{\beta}_1^{-9/7}\tilde{\beta}_4^{(8/7)}\hat{F} + (1 - \tfrac{4}{9}G'^{-7/3}G'' + \tfrac{3}{2}G'''G'^{-5/2} - \tfrac{15}{4}G''^2G'^{-7/2})\hat{F}_\xi \\ +(\tfrac{1}{3}G'^{-4/3} + 3G'^{-5/2}G'')\hat{F}_{\xi\xi} - G'^{-3/2}\hat{F}_{\xi\xi\xi} = 0.\end{aligned} \tag{3.81}$$

With $\hat{\sigma} = O(1)$ as determined before, it is clear that the first term in (3.81) can be dropped to give us a second-order differential equation for $\hat{F}_\xi$. In order to match to the behaviour of $\hat{F}^0_\chi$ as $\chi \to \chi_{\mathrm{p}}$, it is necessary that as $\xi \to \infty$,

$$\hat{F}_\xi \to \tilde{D}\xi^{-7/4} \tag{3.82}$$

for some constant $\tilde{D}$. It is clear that in addition to the behaviour (3.82), equation (3.81) allows transcendental correction in the form (3.78), as for the steady-state

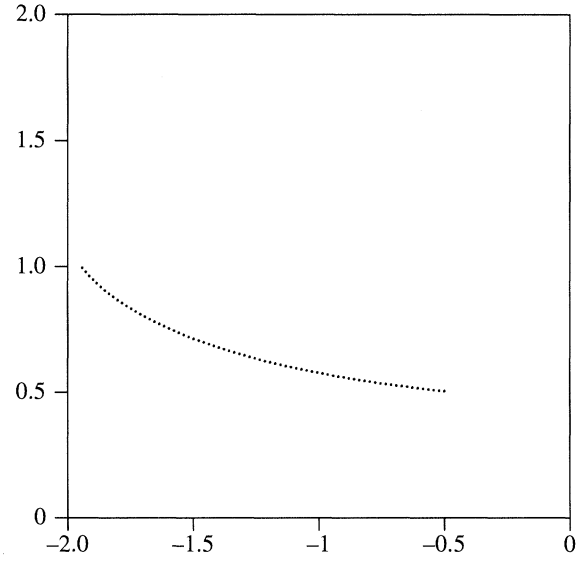

Figure 6. Anti-Stokes line associated with (3.79) that approaches positive Re χ-axis for large $|\chi|$.

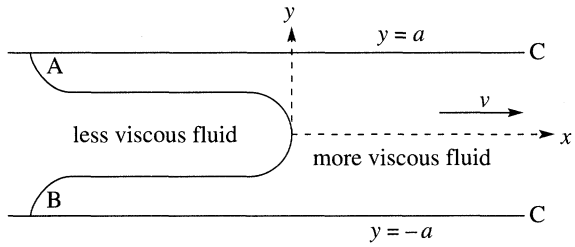

Figure 7. Interface in the z-plane for the time evolving flow.

function $F^{0'}$. Thus, if we integrate (3.81) (simplified by dropping the $\hat{\sigma}$ term), towards $\xi = 0$, using the asymptotic boundary condition (3.82) to obtain $\hat{F}_\chi$ and $\hat{F}_{\chi\chi}$ at an initial point $\xi = \bar{L}$ for large $\bar{L}$, a solution $\hat{F}_\xi$ to (3.81) can be found such that a transcendentally large term of the form (3.78) is suppressed for the large positive ξ-axis. As for the steady state, the absence of such a transcendental term means that transcendental correction of the form (3.62) will be appropriately absent, thus ensuring the validity of (3.49) without any additional constraint on $\hat{\sigma}$.

4. Initial value problem

For the time evolving Hele–Shaw interface, we find it more convenient to use the formulation developed (Tanveer 1993) for the MS boundary conditions. In accordance with this earlier work on the evolution problem, the velocity V of the displaced fluid far ahead of the interface is assumed to be constant. All velocities are scaled by V and all lengths by a, which is at variance with scalings in §§ 2–3. Further, the mathematical formulation is a little different than what is presented in § 2.

Consider the conformal map $z(\zeta, t)$ that maps the unit semicircle in the ζ-plane into the physical flow domain in the z-plane, as shown in figure 7. Notice that unlike

the steady state finger, the interface does not extend to $x = -\infty$. To make the mapping function unique, we require that $\zeta = 0$ correspond to $z = +\infty$ and that $\zeta = \pm 1$ correspond to points A and B in figure 7. It is clear that we can decompose

$$z(\zeta, t) = -\frac{2}{\pi} \ln \zeta + \mathrm{i} + f(\zeta, t), \tag{4.1}$$

where f is analytic in the unit circle with

$$\operatorname{Im} f = 0, \tag{4.2}$$

on the real diameter of the unit circle, which follows from the geometric condition that the side walls of the channel correspond to the real diameter of the unit semicircle. We will assume f is continuous up to the real diameter, including $\zeta = 0$. Further, we assume that the shape of the extended finger obtained by reflection about each of the two side walls is smooth, implying that on the semicircular arc $|\zeta| = 1$, z, and hence f, is analytic and $z_\zeta \neq -0$ inside and on the semicircle. From the Schwartz reflection principle, f is analytic and $z_\zeta \neq 0$ for $|\zeta| \leqslant 1$. We decompose the velocity potential as

$$W(\zeta, t) = -\frac{2}{\pi} \ln \zeta + \mathrm{i} + \omega(\zeta, t). \tag{4.3}$$

It is clear that the condition of no flow through the walls implies that

$$\operatorname{Im} \omega = 0. \tag{4.4}$$

As is physically reasonable, ω will be assumed to be continuous up to the real diameter, including $\zeta = 0$. Further, it will be assumed that ω is analytic on the semicircle, which corresponds to a smooth flow at the interface. From the Schwartz reflection principle, (4.4) implies that ω is analytic in $|\zeta| \leqslant 1$.

The boundary conditions in the laboratory frame can now be written as

$$\operatorname{Re} \omega = -\frac{\epsilon}{3\, Ca_{\mathrm{v}}} \kappa, \tag{4.5}$$

$$\operatorname{Re}\left[\frac{z_t}{\zeta z_\zeta}\right] = \frac{\operatorname{Re}[\zeta W_\zeta]}{|z_\zeta|^2 [1 - m]}, \tag{4.6}$$

where Ca_{v} is the capillary number based on the fluid velocity at $z = +\infty$ and is given by

$$Ca_{\mathrm{v}} = \mu V / T. \tag{4.7}$$

Further, in (4.5) and (4.6),

$$m = m^0(Ca_{\mathrm{v}}\, U_{\mathrm{n}}) + \epsilon \bar{C} m^1(Ca_{\mathrm{v}}\, U_{\mathrm{n}}), \tag{4.8}$$

$$\kappa = \kappa^0(Ca_{\mathrm{v}}\, U_{\mathrm{n}}) + \epsilon \bar{C} \kappa^1(Ca_{\mathrm{v}}\, U_{\mathrm{n}}), \tag{4.9}$$

$$U_{\mathrm{n}} = -\frac{1}{|z_\zeta|} \operatorname{Re}[\zeta^* z_\zeta^* z_t], \tag{4.10}$$

$$\bar{C} = -\frac{1}{|z_\zeta|} \operatorname{Re}\left[1 + \frac{\zeta z_{\zeta\zeta}}{z_\zeta}\right]. \tag{4.11}$$

The analytical continuation of U_{n} and $\bar{C}$ off the circular arc is given by

$$U_{\mathrm{n}}(\zeta, t) = -\frac{1}{2 z_\zeta^{1/2} [z_\zeta(1/\zeta, t)]^{1/2}} \left[\frac{1}{\zeta} z_\zeta\left(\frac{1}{\zeta}, t\right) z_t + \zeta z_\zeta z_t\left(\frac{1}{\zeta}, t\right)\right], \tag{4.12}$$

$$\bar{C}(\zeta,t) = -\frac{1}{z_\zeta^{1/2} z_\zeta^{1/2}(1/\zeta,t)}\left[1 + \frac{1}{2}\frac{\zeta z_{\zeta\zeta}}{z_\zeta} + \frac{1}{2}\frac{z_{\zeta\zeta}(1/\zeta,t)}{\zeta z_\zeta(1/\zeta,t)}\right]. \tag{4.13}$$

The analytical continuation of the kinematic and dynamic conditions outside the unit circle gives us

$$\frac{z_t}{\zeta z_\zeta} = \mathcal{I}\left[\frac{\mathrm{Re}[\zeta W_\zeta]}{|z_\zeta|^2[1-m]}\right] + \frac{[-4/\pi + \zeta\omega_\zeta + (1/\zeta)\omega_\zeta(1/\zeta)]}{z_\zeta z_\zeta(1/\zeta,t)[1-m]}, \tag{4.14}$$

$$\omega = -\frac{\epsilon}{3\,Ca_\mathrm{v}}\mathcal{I}[\kappa] - \frac{2\epsilon}{3\,Ca_\mathrm{v}}\kappa, \tag{4.15}$$

where the integral operator $\mathcal{I}$ is now defined by

$$\mathcal{I}(g) = \int_0^{2\pi} \mathrm{d}\nu' \frac{\zeta + \mathrm{e}^{\mathrm{i}\nu'}}{\mathrm{e}^{\mathrm{i}\nu'} - \zeta} g(\mathrm{e}^{\mathrm{i}\nu'}). \tag{4.16}$$

(*a*) *Dynamics for* $\epsilon = 0$

First we consider the case of $\epsilon = 0$. In that case, $\omega = 0$ and (4.14) simplifies to

$$z_t^0 = q_1^0 z_\zeta^0 + q_2^0, \tag{4.17}$$

where

$$q_1^0 = \zeta I_4^0,$$

where

$$I_4^0 = -\frac{1}{\pi^2\mathrm{i}}\oint_{|\zeta'|=1}\frac{\mathrm{d}\zeta'}{\zeta'}\left[\frac{\zeta+\zeta'}{\zeta'-\zeta}\right]\frac{1}{[1-m^0(Ca_\mathrm{v}\,U_\mathrm{n}(\zeta',t)]|z_\zeta(\zeta',t)|^2} \tag{4.18}$$

and

$$q_2^0(\zeta,t) = -\frac{2}{\pi}\frac{2\zeta}{(1-m^0(Ca\,U_\mathrm{n}(\zeta,t))\tilde{z}_\zeta(\frac{1}{\zeta},t)}. \tag{4.19}$$

Further, note from (4.18) that for $|\zeta| < 1$, $\mathrm{Re}\, I_4^0$ defines a harmonic function so that on $|\zeta| = 1$,

$$\mathrm{Re}\, I_4^0(\zeta,t) = -\frac{1}{(1-m^0(Ca\,U_\mathrm{n}(\zeta,t))|z_\zeta(\zeta,t)|^2}\frac{2}{\pi}. \tag{4.20}$$

Thus, from the maximum principle for a harmonic function in $|\zeta| < 1$,

$$\max_{|\zeta|=1}\frac{2}{\pi}\frac{1}{(1-m^0(Ca\,U_\mathrm{n})|z_\zeta|^2} > -\mathrm{Re}\, I_4^0 > \min_{|\zeta|=1}\frac{2}{\pi}\frac{1}{(1-m^0(Ca\,U_\mathrm{n}))|z_\zeta|^2} > 0. \tag{4.21}$$

Further, after a little manipulation of (4.18), we get

$$I_4^0\left(\frac{1}{\zeta_1},t\right) = \frac{1}{\pi^2\mathrm{i}}\oint_{|\zeta'|=1}\frac{\mathrm{d}\zeta'}{\zeta'}\left[\frac{\zeta_1+\zeta'}{\zeta'-\zeta_1}\right]\frac{1}{(1-m^0(1/\zeta',t))|z_\zeta(1/\zeta',t)|^2}, \tag{4.22}$$

where $m^0(1/\zeta,t)$ denotes the evalution of $m^0(Ca\,U_\mathrm{n})$ with $1/\zeta$ replacing ζ in the expression for U_n in (4.12). It is clear that $\mathrm{Re}\, I_4(1/\zeta_1,t)$ is a harmonic function in $|\zeta_1| < 1$, taking on the boundary value

$$\mathrm{Re}\, I_4^0\left(\frac{1}{\zeta_1},t\right) = \frac{1}{(1-m^0(1/\zeta_1,t))|z_\zeta(1/\zeta_1,t)|^2}\frac{2}{\pi} \tag{4.23}$$

PHILOSOPHICAL TRANSACTIONS OF THE ROYAL SOCIETY A MATHEMATICAL, PHYSICAL & ENGINEERING SCIENCES

on $|\zeta_1| = 1$. By putting $\zeta_1 = 1/\zeta$, from the maximum principle, it follows that for any $|\zeta| > 1$,

$$\max_{|\zeta|=1} \frac{1}{(1-m^0)|z_\zeta|^2}\frac{2}{\pi} > \mathrm{Re}\, I_4^0 > \min_{|\zeta|=1} \frac{1}{(1-m^0)|z_\zeta|^2}\frac{2}{\pi} > 0. \tag{4.24}$$

The last inequality in (4.24) holds up to the time when a strong singularity $|z_\zeta|$ impinges $|\zeta| = 1$, if indeed it does so. The properties above will be crucial in showing that an initial singularity in $|\zeta| > 1$ continually travels towards the boundary of the physical domain $|\zeta| = 1$, though it need not always impinge it.

For further analysis of (4.17), it is helpful to remove z_t appearing explicitly in (4.19) through the argument U_n of m^0, where U_n is given by (4.12). In order to do so, we exploit the identity

$$q_1^0(\zeta, t) = -\zeta^2 \frac{z_t(1/\zeta, t)}{z_\zeta(1/\zeta, t)} \tag{4.25}$$

that can be found from (4.6) by using Poisson integral formulae for a harmonic function and its conjugate where $|\zeta^{-1}| < 1$. Then, on using (4.17), it is seen that expression (4.12) for U_n can be replaced by

$$U_\mathrm{n} = -\frac{z_\zeta^{1/2}(\zeta^{-1}, t) q_2^0(\zeta, t)}{2\zeta z_\zeta^{1/2}}. \tag{4.26}$$

Substituting (4.26) back into (4.19), we have an implicit representation of q_2^0 given by

$$q_2^0 \left[1 - m^0\left(-Ca_\mathrm{v}\, q_2^0 \frac{z_\zeta^{1/2}(\zeta^{-1}, t)}{2\zeta z_\zeta^{1/2}}\right)\right] = -\frac{4\zeta}{\pi z_\zeta(\zeta^{-1}, t)}. \tag{4.27}$$

The analysis of the general properties of the solution to the integro-differential equation (4.17) is not possible at this stage as it involves knowledge of the function m^0 for arbitrary complex arguments. So far, Reinelt's (1987*a*) numerical calculation is limited to real and positive arguments. If m^0 in (4.18) and (4.27) are ignored, which is only appropriate as $Ca_\mathrm{v} \to 0$, we recover the $\mathcal{B} = 0$ problem of the MS boundary contitions†. The general properties of this and other equivalent integro-differential equations for the MS boundary conditions have been explored before (see the reviews of Howison (1992) and Hohlov *et al.* (1994) in addition to Tanveer (1993)). Despite the difficulty in the analysis of (4.17) in the presence of m^0, we note some interesting properties. As with the theory (Tanveer 1993) with MS conditions, q_1^0 in (4.17) is clearly analytic for all $|\zeta| > 1$, except at infinity, where it is proportional to ζ. However, unlike the MS case, the same is not true for q_2^0. The presence of the m^0 term in (4.27) can cause q_2^0 to be singular in $|\zeta| > 1$ at values of ζ because of the following possibilities: (i) z_ζ is singular and blows up; (ii) $1 - m^0$ approaches zero; (iii) z_ζ approaches zero; (iv) the argument of m^0 approaches a possible singularity of the function m^0. The possibilities (ii)–(iv) are interesting, but cannot be confirmed because of our limited knowledge of m^0. We only explore possibility (i). First, we note that for $|\zeta| > 1$, $z_\zeta(\zeta^{-1}, t)$ is both analytic and non-zero. Thus, as we approach

† $\mathcal{B}$ is proportional to $\epsilon^2/(Ca_\mathrm{v})$ and so there is an equilavency between zero surface tension and zero ϵ for the MS conditions, unlike the present problem

a singular point of z_ζ (where z_ζ grows without bounds), it is clear that if q_2^0 is finite, then from (4.26), the argument of m^0 becomes small, regardless of whether Ca is small or not. Thus, Bretherton's approximation (2.6), assumed to be valid for small complex arguments, gives us

$$q_2^0 \sim -\frac{4\zeta}{\pi z_\zeta(\zeta^{-1},t)}[1+1.3375\ Ca_{\rm v}^{2/3}\ z_\zeta^{-1/3}(\zeta^{-1},t)z_\zeta^{-1/3}2^{2/3}\pi^{-2/3}]. \tag{4.28}$$

The *a priori* assumption that q_2^0 is finite at $\zeta=\zeta_{\rm s}$ is verified *a posteriori*, since the second term in the square parentheses in (4.28) is clearly zero at that point. From (4.26) and (4.28),

$$U_{\rm n} \sim \frac{2}{\pi} z_\zeta^{-1/2}(\zeta^{-1},t)z_\zeta^{-1/2}\left[1+1.3375\ Ca_{\rm v}^{2/3}\ z_\zeta^{-1/3}(\zeta^{-1},t)\right]. \tag{4.29}$$

Consider an initial singularity of z_ζ at $\zeta_{\rm s}(0)$, such that as $\zeta\to\zeta_{\rm s}(0)$

$$z(\zeta,0) \sim A_0(0) + \frac{A_{s_1}(0)}{1-\beta}(\zeta-\zeta_{\rm s}(0))^{(1-\beta)}+\cdots, \tag{4.30}$$

with $3>\beta>\frac{3}{4}$ and $\beta\neq\frac{3}{2}$. We seek a solution $z(\zeta,t)$ to (4.17) such that it admits a moving singularity $\zeta_{\rm s}(t)$ that initially coincides with $\zeta_{\rm s}(0)$. Assuming such a solution exists, near the singularity, we seek a local expansion of the type

$$z(\zeta,t) \sim A_0(t) + \frac{A_{s_1}(t)}{1-\beta}(\zeta-\zeta_{\rm s}(0))^{(1-\beta)} + B_{\rm s}(t)(\zeta-\zeta_{\rm s}(t))^{\beta/3}+\cdots \tag{4.31}$$

for small $|\zeta-\zeta_{\rm s}(t)|$. It is to be noted that, depending on the value of β, the term $(\zeta-\zeta_{\rm s}(t))^{\beta/3}$ can actually be subdominant to a term of the type $A_{s_2}(\zeta-\zeta_{\rm s}(t))^{(2-\beta)}$, which is left out of (4.31). Since there is no interaction between these two terms except for the special case $2-\beta=\frac{1}{3}\beta$, which is excluded in this analysis, we will ignore the $(\zeta-\zeta_{\rm s})^{2-\beta}$ term. Then, on substitution of (4.31) into (4.17), after using the asymptotic expansion (4.28), we find consistency, provided

$$\dot{A}_0 = D_0(t), \tag{4.32}$$

$$\dot{\zeta}_{\rm s} = -q_1^0(\zeta_{\rm s}(t),t), \tag{4.33}$$

$$\dot{A}_{s_1} = (1-\beta)q_{1\zeta}^0(\zeta_{\rm s}(t),t)A_{s_1}, \tag{4.34}$$

$$\dot{B}_{\rm s} = D_1(t)A_{s_1}^{-1/3}(t), \quad \text{with } B_{\rm s}(0)=0, \tag{4.35}$$

where

$$D_0(t) = -\frac{4\zeta_{\rm s}(t)}{\pi z_\zeta(\zeta_{\rm s}^{-1}(t),t)}, \tag{4.36}$$

$$D_1(t) = -\frac{4\zeta_{\rm s}(t)(1.3375)\ Ca_{\rm v}^{2/3}\ 2^{2/3}}{\pi^{5/3}z_\zeta^{4/3}(\zeta_{\rm s}^{-1}(t),t)}. \tag{4.37}$$

It appears there is no problem in carrying out term-by-term matching of the progressively less singular terms; however, if the relations are truncated at any stage, there are not enough equations to find all the unknowns. This is to be expected because of the global nature of the dynamics in (4.17).

Nonetheless, from relation (4.29), we find that a singularity $\zeta_{\rm s}(t)$ of the the type considered here, moves with speed $-q_1^0(\zeta_{\rm s}(t),t)$. The presence of $1-m^0$ term in

the denominator in (4.18) distinguishes it from the expression of the the singularity speed (Tanveer 1993) corresponding to the MS boundary conditions. We note that from (4.18), (4.24) and (4.33),

$$\mathrm{Re}\left[\frac{\dot{\zeta}_s}{\zeta_s}\right] = -\,\mathrm{Re}\, I_4^0(\zeta_s, t) < 0. \tag{4.38}$$

The left-hand side of (4.38) is simply $\dot{R}/R$, where $\zeta_s(t) = R(t)e^{i\nu_s(t)}$. So (4.38) implies that $\dot{R} < 0$ and that a singularity continually moves inwards towards the the physical domain boundary $|\zeta| = 1$. The analytical arguments put forward before (see Tanveer (1993), § 3), suggesting that singularities of this type where $\beta \geqslant \frac{1}{2}$ cannot impinge the physical domain boundary $|\zeta| = 1$ in finite time, can be repeated, almost without any alteration, since, to the leading order, $1/(1-m^0)$ is merely a constant at such a singularity $\zeta_s(t)$.

Now, let us consider initial singularities of the type (4.30) with $0 < \beta < \frac{3}{4}$. In this case, it is to be noted that (4.31) cannot be valid. In that case, the early time $t \ll 1$ behaviour of a solution to (4.17) near the singularity is given by a similarity solution. For $\zeta - \zeta_s(t) = O(t^{3/(3-4\beta)})$, $t \ll 1$, the solution is given by

$$z \sim A_0(0) + t^{(3-3\beta)/(3-4\beta)} k^{1-\beta} F(\eta) + \cdots, \tag{4.39}$$

$$\eta = \frac{\zeta - \zeta_s(t)}{k t^{3/(3-4\beta)}}, \tag{4.40}$$

where k is a constant determined by

$$-\frac{4\zeta_s(t)}{3\pi z_\zeta(\zeta_s^{-1}(t), t)}[1.3375\, Ca_v^{2/3}\, z_\zeta^{-1/3}(\zeta_s^{-1}(t), t) 2^{2/3}\pi^{-2/3}](3-4\beta)k^{4\beta/3-1}A_{s_1}^{-4/3}(0) = 1, \tag{4.41}$$

and the function $F(\eta)$ is a solution to

$$(1-\beta)F - \eta F' = F'^{-1/3}, \tag{4.42}$$

that satifies the asymptotic condition

$$F \sim \frac{\eta^{1-\beta}}{(1-\beta)} \tag{4.43}$$

as $|\eta| \to \infty$. Equation (4.42) admits singularities of the type $(\eta - \eta_0)^{3/4}$. The implication of a similarity solution (4.39) that allows such singularities is that initial singularities in the form (4.30) with $0 < \beta < \frac{3}{4}$ immediately transform into one or more singularities with $\beta = \frac{3}{4}$, which is known not to impinge $|\zeta| = 1$ in finite time as it comes indefinitely close. This feature of the dynamics is different from that of the $\mathcal{B} = 0$ (or $\epsilon = 0$) problem with MS boundary conditions, where the nature of the singularity is preserved, regardless of its nature.

We now consider a weaker initial singularity $\zeta_s(0)$, such that as $\zeta \to \zeta_s(0)$,

$$z(\zeta, 0) = A_0(0) + A_1(0)(\zeta - \zeta_s(0)) + \frac{A_{s_1}(0)}{1+\beta}(\zeta - \zeta_s(0))^{1+\beta} + \cdots, \tag{4.44}$$

with $\beta > 0$. In this case, an expansion of the type

$$z(\zeta, t) = A_0(t) + A_1(t)(\zeta - \zeta_s(t)) + \frac{A_{s_1}(t)}{1+\beta}(\zeta - \zeta_s(t))^{1+\beta} + \cdots \tag{4.45}$$

PHILOSOPHICAL TRANSACTIONS OF THE ROYAL SOCIETY A MATHEMATICAL, PHYSICAL & ENGINEERING SCIENCES

is consistent with (4.17) for $t > 0$, provided

$$\dot{\zeta}_s = -q_1^0(\zeta_s(t), t) + q_2^s(t), \tag{4.46}$$

where $q_2^s(t)$ is determined from

$$\frac{q_2^s(t)}{q_2^0(\zeta_s(t), t)} = \frac{Ca_v\, m^{0'}(Ca_v\, U_n^0(t)) z_\zeta^{1/2}(\zeta_s^{-1}(t), t)}{2\zeta_s(t)[1 - m^0(Ca_v\, U_n^0(t))]} [A_1^{-1/2} q_2^s(t) - \tfrac{1}{2} A_{s_1} q_2^0(\zeta_s(t), t) A_1^{-3/2}], \tag{4.47}$$

where $q_2^0(\zeta_s(t), t)$ is implicitly determined by

$$q_2^0(\zeta_s(t), t)[1 - m^0(-\tfrac{1}{2}\, Ca_v\, z_\zeta^{1/2}(\zeta_s^{-1}(t), t) q_2^0(\zeta_s(t), t) A_1^{-1/2} \zeta_s^{-1}(t))] = -\frac{4\zeta_s(t)}{\pi z_\zeta(\zeta_s^{-1}(t), t)}, \tag{4.48}$$

where $U_n^0(t)$ is determined by (4.29) with $\zeta = \zeta_s(t)$. In this case, the singularity does not move with $-q_1$, as before. However, it is clear from the Bretherton approximation (2.6) that for small Ca_v, q_2^s is going to be small, in which case the singularity speed ζ_s approaches $-q_1$. Even when Ca_v is not very small, so that (2.6) is invalid, the property $\mathrm{Re}[\dot{\zeta}_s(t)/\zeta_s(t)] < 0$ will hold provided

$$\mathrm{Re}[q_1(\zeta_s(t), t)/\zeta_s(t)]$$

is larger in absolute value than $\mathrm{Re}[q_2^s(t)/\zeta_s(t)]$, which is expected for moderately small Ca_v. Note that in this case, because the singularity is weak and $1/(z_\zeta(\zeta_s(t), t))$ remains bounded, the singularity does not slow down as it approaches $|\zeta| = 1$, unlike the case in (4.31). Consequently, $\zeta_s(t)$ impinges the boundary $|\zeta| = 1$ of the physical domain in finite time, leading to a curvature singularity.

This corresponds to an ill-posed dynamics in the physical domain $|\zeta| \leqslant 1$ in any Sobolev norm that measures the curvature of the interface, as we now argue. Consider two initial conditions, say

$$z^1(\zeta, 0) = -\frac{2}{\pi} \ln \zeta + 0.1\zeta \tag{4.49}$$

and

$$z^2(\zeta, 0) = -\frac{2}{\pi} \ln \zeta + 0.1\zeta + \delta^n(\zeta^2 + 1 + \delta)^{4/3}, \tag{4.50}$$

where δ and n are each greater than zero, with $\delta < 1$. Clearly, for any given Sobolev norm defined on the interface $|\zeta| = 1$, the difference between the two initial conditions can be made arbitrarily small by either choosing n sufficiently large or δ sufficiently small. Yet, as time evolves, prior discussion suggests that the singularity formed in these initial conditions will be preserved and that the singularities $(\zeta - \zeta_s(t))^{4/3}$ in the second case will impinge $|\zeta| = 1$. The time at which this singularity impinges can be controlled and made arbitrarily small by choosing δ small. In a Sobolev norm that accounts for the interfacial curvature, the $\epsilon = 0$ evolution problem is therefore ill-posed in the sense of Hadamard, since clearly the difference of the two solutions measured at the interface $|\zeta| = 1$ can be made $O(1)$ in arbitrarily short time. It is unclear at this stage if the ill-posedness is also in the sense that interface slopes for two different initial conditions can deviate by $O(1)$ in arbitrarily short time even when they start out close. This appears to be resolvable only by examining details of the function m^0 not available so far.

(*b*) *Effect of small non-zero* ϵ

Now, let us consider the effect of introduction of a small non-zero ϵ. This can be done effectively by studying the problem perturbatively in the extended domain $|\zeta| > 1$, where the dynamics of the $\epsilon = 0$ can be expected to be well posed, following earlier findings for the MS boundary conditions (Tanveer 1993; Baker *et al.* 1994). Here, we restrict ourselves to what happens to an initial singularity of the type (4.30) with $2 > \beta > \frac{3}{4}$.

As in Tanveer (1993), it is convenient to introduce inner variables

$$\zeta - \zeta_s(t) = \mathcal{B}^{2/(3(2-\beta))} \frac{1}{C_0(t)} \chi, \tag{4.51}$$

$$z_\zeta = \mathcal{B}^{-2\beta/(3(2-\beta))} C_0(t) G(\chi, \tau), \tag{4.52}$$

$$\tau = \int_0^t \mathrm{d}t\, C_0^{3/2}(t) q_{7^0}(\zeta_s(t), t), \tag{4.53}$$

where

$$q_7^0(\zeta, t) = -\frac{\zeta^3}{z_\zeta^0(\zeta^{-1}, t)}, \tag{4.54}$$

$$C_0(t) = C_0(0) \exp\left(\int_0^t \mathrm{d}t'\, q_{1^0\zeta}(\zeta_s(t'), t') \right), \tag{4.55}$$

where

$$\mathcal{B} = \frac{\pi}{4} \frac{\epsilon^2}{3\, Ca_v}. \tag{4.56}$$

It is to be noted that the definition of $\mathcal{B}$ here is different from Tanveer (1993) by a factor of $\frac{1}{4}\pi$ to account for the observation of Reinelt (1987*b*) that the boundary condition with the thin-film effects only asymptotes to the MS boundary condition for $\epsilon \ll Ca \ll 1$ provided the effective lumped parameter $\mathcal{B}$ is chosen to be a factor of $\frac{1}{4}\pi$ different from that with the MS. Further, note that in order for (4.52) to be consistent with (4.30), $C_0(0)$ has to be related to $A_{s_1}(0)$. On substituting the above relation into (4.51)–(4.55) and back into (4.14) and (4.15), we find that the the leading-order equation in the asympotic limit $\mathcal{B} \to 0$ with $\chi = O(1)$ is

$$G_\tau = -2 \frac{\partial^3}{\partial \chi^3} G^{-1/2}. \tag{4.57}$$

In deriving the above, we assumed $|\zeta_s(t)| - 1 \gg \mathcal{B}^{2/(3(2-\beta))}$, or otherwise the inner equation is an integro-differential equation. Equation (4.57) is the so-called Harry–Dym equation that arises frequently in the theory of integrable partial differential equations. However, our interest in (4.57) is in complex solutions where integrable theory does not apply. Within the context of MS boundary conditions, It was recognized (Kadanoff, personal communication; Howison 1992; Tanveer 1993) that this equation has a similarity solution of the form

$$G(\chi, \tau) = \tau^{-(2\beta)/(3(2-\beta))} \tilde{F}(\tau^{-2/(3(2-\beta))} \chi). \tag{4.58}$$

Tanveer (1993) pointed out that such solutions can be matched to the outer solution that behaves like (4.31) near $\zeta = \zeta_s$ along certain sectors of the complex plane that are relevant to physical domain dynamics. Further, this solution only admits $-\frac{4}{3}$ singularities.

From the definition of the variables given in (4.51)–(4.53) and the form of the similarity solution, it is clear that an initial singularity in the form $(\zeta - \zeta_s(0))^{-\beta}$ is immediately transformed into an inner structure that scales like the product of $\mathcal{B}t$, within which possibly multiple $-\frac{4}{3}$ singularities reside. The centre of this structure is at $\zeta_s(t)$, which moves towards $|\zeta| = 1$ (i.e. towards the physical interface) according to the $\epsilon = 0$ dynamics described in the last subsection. Since, as argued earlier, such singularities do not impinge the physical domain in finite time and only approach it exponentially (Tanveer 1993), if the initial singularity distance is $O(1)$ from the interface $|\zeta| = 1$, it would take a long time of $O(-\ln \mathcal{B})$ before $|\zeta_s(t)| - 1 = O(\mathcal{B}^{2/3(2-\beta)})$, when non-zero ϵ effects as in (4.51)–(4.53) can affect the physical interface $|\zeta| = 1$. Before such time, the observed interfacial dynamics will essentially be the same as for $\epsilon = 0$. For the MS boundary conditions, the $\epsilon = 0$ (equivalent to $\mathcal{B} = 0$ problem) dynamics have been studied by Baker *et al.* (1994) for a general class of initial conditions that include branch points as in (4.30); it has been shown that the proximity of such singularities to $|\zeta| = 1$ describes many different patterns of tip-splitting and side branching that depend on the initial distribution of singularities. Our study here shows that these dynamics are indeed relevant when realistic three-dimensional effects are included, provided $\frac{3}{4} < \beta < 2$, since for a long time, the condition $1 \gg |\zeta_s(t)| - 1 \gg \mathcal{B}^{2/3(2-\beta)}$, necessary for interface indentation to be significant as well as similar to that for $\epsilon = 0$, holds.

To the extent that there is no serious loss of generality in assuming analytic initial conditions on $|\zeta| = 1$, the extreme sensitivity in the experimentally observed dynamics can be traced back merely to the observation that the initial interface shape determined up to some finite precision can correspond to many different singularity distributions of $z(\zeta, t)$ in $|\zeta| > 1$; yet at later times, when such singularities approach $|\zeta| = 1$, the observed interface deformation is different in each case. Further, for a generic initial condition $z(\zeta, 0)$ specified in $|\zeta| \leqslant 1$, it can be expected that the analytically continued initial condition in $|\zeta| > 1$ will have infinitely many singularities $\zeta_s(0)$ at arbitrarily large distance from $|\zeta| = 1$. Yet, the continual approach of the resulting inner structures associated with each $\zeta_s(t)$ towards $|\zeta| = 1$ will result in a continually evolving interface that cannot settle to any steady state. This qualitatively explains the observed dynamics in the experiment.

5. Discussion and conclusion

In this paper, we have included three-dimensional thin-film effects on unsteady Hele–Shaw fingering of a viscous fluid by a less viscous fluid of negligible viscosity. Through a formal calculation involving asymptotics beyond all orders, we have shown that, as with the theory with idealized MS boundary conditions that ignore thin-film effects, only one branch of the steady-state solution, the one for which the finger width is the smallest, is linearly stable in the asymptotic limit $\epsilon \ll Ca \ll 1$.

Further, in a limited sense, we have also only considered the nonlinear initial value problem without any restriction on Ca but with $\epsilon \ll 1$. It has been shown that when lateral curvature effects (i.e. $\epsilon = 0$) are completely neglected, then many types of initial singularities present in the extended unphysical domain $|\zeta| > 1$ continually move towards the physical interface corresponding to $|\zeta| = 1$. While some of these singularities never impinge the physical domain in finite time, others that correspond to a weaker curvature singularity do. This leads to an ill-posedness of the initial value problem when $\epsilon = 0$ for Sobolev norms that account for interfacial curvature. For

PHILOSOPHICAL TRANSACTIONS OF THE ROYAL SOCIETY A MATHEMATICAL, PHYSICAL & ENGINEERING SCIENCES

certain forms of singularities, the effect of a small non-zero ϵ is felt only locally in small neighbourhoods of singularities (in $|\zeta| > 1$) of the $\epsilon = 0$ problem, where initial singularities are possibly transformed into one or more $-\frac{4}{3}$ singularities. Nonetheless, the centre of such an inner structure, to the leading order, moves like a singularity of the $\epsilon = 0$ problem until it comes very close to $|\zeta| = 1$. Since in some cases the $\epsilon = 0$ singularities do not impinge the physical domain in finite time and only approach it exponentially, there exists a long time where the interfacial shapes and distortions correspond to that for the $\epsilon = 0$ problem. This helps explain the apparently random continual time evolving pattern observed in experiment for sufficiently small ϵ. To the extent that aggregate features of the experimentally observed dynamics do not critically depend on our assumption that the initial interface shape be analytic, it would be interesting to determine statistical features of the interface shapes with a random collection of initial singularities in $|\zeta| > 1$.

This research was primarily supported by the Department of Energy (DE-FG02-92ER14270) and the National Science Foundation (NSF DHS-9500986). The author is also grateful to the Isaac Newton Institute (Exponential Asymptotics program) for support during the final completion stage of this paper. The author is also thankful to the referees for helpful comments.

References

Arneodo, A., Couder, Y., Grasseau, G., Hakim, V. & Rabaud, M. 1989 Uncovering the analytical Saffman–Taylor finger in unstable viscous fingering and diffusion limited aggregation. *Phys. Rev. Lett.* **63**, 984.

Baker, G. & Tanveer, S. 1992 Well posed numerical calculations for free-surface flows. In *NATO ARW Proc. on Singularities in Fluids, Plasmas and Optics* (ed. R. Caflisch & G. Papanicolau). Amsterdam: Kluwer.

Bensimon, D., Kadanoff, L. P., Liang, S., Shraiman, B. I. & Tang, C. 1986 Viscous flows in two dimensions. *Rev. Mod. Phys.* **58**, 977.

Bensimon, D. 1986 Stability of viscous fingering. *Phys. Rev.* A **33**, 1302.

Bensimon, D., Pelce, P. & Shraiman, B. I. 1987 Dynamics of curved front and pattern selection. *J. Physique* **48**, 2081.

Berry, M. V. 1991 Asymptotics, superasymptotics, hyperasymptotics. In *NATO ARW Proc. on Asymptotics beyond all orders* (ed. H. Segur, S. Tanveer & H. Levine).

Bretherton, F. P. 1961 The motion of long bubbles in tubes. *J. Fluid Mech.* **10**, 166.

Combescot, R., Dombre, T., Hakim, V., Pomeau, Y. & Pumir, A. 1986 Shape selection for Saffman–Taylor fingers. *Phys. Rev Lett.* **56**, 2036.

Combescot, R., Dombre, T., Hakim, V., Pomeau, Y. & Pumir, A. 1987 Analytic theory for the Saffman–Taylor fingers. *Phys. Rev.* A **37**, 1270.

DeGregoria, A. J. & Schwartz, L. W. 1986 A boundary-integral method for two-phase displacement in Hele–Shaw cells. *J. Fluid. Mech.* **164**, 383.

Dorsey, A. T. & Martin, O. 1987 Saffman–Taylor fingers with anisotropic surface tension. *Phys. Rev.* A **35**, 3989.

Hohlov, Y. E., Howison, S. D., Huntingford, C., Ockendon, J. R. & Lacey, A. A. 1994 A model for non-smooth free boundaries in Hele–Shaw flows. *Q. Jl Mech. Appl. Math.* **47**, 107.

Hong, D. C. & Langer, J. S. 1986 Analytic theory for the selection of Saffman–Taylor finger. *Phys. Rev. Lett.* **56**, 2032.

Homsy, G. M. 1987 Viscous fingering. *A. Rev. Fluid Mech.* **19**, 271.

Howison, S. D. 1986*a* Fingering in Hele–Shaw cells. *J. Fluid Mech.* **167**, 439.

Howison, S. D. 1986*b* Cusp development in Hele–Shaw flow with a free surface. *SIAM Jl Appl. Math.* **46**, 20–26.

Howison, S. D. 1992 Complex variable methods in Hele–Shaw moving boundary problems. *Eur. J. Appl. Math.* **3**, 209.

PHILOSOPHICAL TRANSACTIONS OF THE ROYAL SOCIETY A MATHEMATICAL, PHYSICAL & ENGINEERING SCIENCES

Kessler, D., Koplik, J. & Levine, H. 1988 Patterned selection in fingered growth phenomena. *Adv. Phys.* **37**, 255.

Kessler, D. & Levine, H. 1986 Stability of finger patterns in Hele–Shaw cells. *Phys. Rev.* A **33**, 2632.

Kruskal, M. & Segur, H. 1986 Asymptotics beyond all orders. Aeronautical Res. Associates of Princeton Technical Memo 85-25.

Maxworthy, T. 1987 The nonlinear growth of a gravitationally unstable interface in a Hele–Shaw cell. *J. Fluid Mech.* **177**, 207.

McLean, J. W. & Saffman, P. G. 1981 The effect of surface tension on the shape of fingers in a Hele–Shaw cell. *J.Fluid Mech.* **102**, 455–469.

Meiburg, E. & Homsy, G. M. 1988 Nonlinear unstable viscous fingers in Hele–Shaw flows. II. Numerical simulation. *Physics Fluids* **31**, 429.

Park, C. W. & Homsy, G. M. 1985 Two-phase displacement in Hele–Shaw cells: theory. *J. Fluid Mech.* **139**, 291.

Pelce, P. 1988 *Dynamics of curved front.* New York: Academic.

Pokrovsky, V. L. & Khalatnikov, I. M. 1961 *Soviet Phys. JETP* **13**, 1207.

Reinelt, D. A. 1987*a* Interface conditions for two-phase displacement in Hele–Shaw cells. *J. Fluid Mech* **183**, 219.

Reinelt, D. A. 1987*b* The effect of thin film variations and transverse curvature on the shape of fingers in a Hele–Shaw cell. *Physics Fluids* **30**, 2617.

Saffman, P. G. & Taylor, G. I. 1958 The penetration of a fluid into a porous medium of Hele–Shaw cell containing a more viscous fluid. *Proc. R. Soc. Lond.* A **245**, 312.

Saffman, P. G. & Taylor, G. I. 1959 In *Proc. 2nd A. Naval Symp. Hydrodynamics*, pp. 277. Washington, DC: ONR.

Saffman, P. G. 1959 Exact solution for the growth of fingers from a flat interface between two fluids. *Q. Jl Mech. Appl. Math.* **12**, 146–150.

Saffman, P. G. 1982 *Fingering in porous medium* (ed. Burridge *et al.*), pp. 208. (Springer Lecture Notes in Physics.) Berlin: Springer.

Saffman, P. G. 1986 Viscous fingering in a Hele–Shaw cell. *J. Fluid Mech.* **173**, 73.

Sarkar, S. & Jasnow, D. 1987 Quantitative test of solvability theory for the Saffman–Taylor problem. *Phys. Rev.* A **35**, 4900.

Schwartz, L. W. & Degregoria, A. J. 1987 Simulation of Hele–Shaw cell fingering with finite capillary number effects included. *Phys. Rev.* A **35**, 276.

Shraiman, B. I. 1986 On velocity selection and the Saffman–Taylor problem. *Phys. Rev. Lett.* **56**, 2028.

Shraiman, B. I. & Bensimon, D. 1985 Singularities in nonlocal dynamics. *Phys. Rev.* A **30**, 2840.

Siegel, M., Tanveer, S. & Dai, W. S. 1996 Singular effects of surface tension in a smoothly evolving Hele–Shaw flow. *J. Fluid Mech.* (Submitted.)

Tabeling, P., Zocchi, G. & Libchaber, A. 1987 An experimental study of the Saffman–Taylor instability. *J. Fluid Mech.* **177**, 67.

Tanveer, S. 1987*a* Analytic theory for the selection of symmetric Saffman–Taylor finger. *Physics Fluids* **30**, 1589.

Tanveer, S. 1987*b* Analytic theory for the linear stability of Saffman–Taylor finger. *Physics Fluids* **30**, 2318.

Tanveer, S. 1990 Analytic theory for the selection of Saffman–Taylor finger in the presence of thin-film effects. *Proc. R. Soc. Lond.* A **428**, 511.

Tanveer, S. 1991 Viscous displacement in a Hele–Shaw cell. In *Asymptotics beyond all orders.* (ed. H. Segur, S. Tanveer & H. Levine), NATO ASI series B, vol. 284, New York: Plenum.

Tanveer, S. 1993 Evolution of Hele–Shaw interface for small surface tension. *Phil. Trans. R. Soc. Lond.* A **343**, 155.

Vanden-Broeck, J. M. 1983 Fingers in a Hele–Shaw cell with surface tension. *Physics Fluids* **26**, 2033.

Received 19 November 1993; revised 10 January 1995; accepted 2 August 1995

PHILOSOPHICAL TRANSACTIONS OF THE ROYAL SOCIETY A MATHEMATICAL, PHYSICAL & ENGINEERING SCIENCES